DOI: 10.17277/amt.2018.02.pp.018-041

Functionalization of Carbon Nanotubes: Methods, Mechanisms and Technological Realization

T.P. Dyachkova*, A.V. Rukhov, A.G. Tkachev, E.N. Tugolukov

Tambov State Technical University,
106, Sovetskaya St., Tambov, 392000, Russia

*Corresponding author: Tel.: +7 4752 63 55 22. *E-mail*: dyachkova_tp@mail.ru

Abstract

The paper considers the main regularities of liquid-phase and gas-phase functionalization of carbon nanotubes. The effective values of the kinetic parameters (rate constants and activation energy) of the processes occurring during various types of chemical treatment of carbon nanotubes were determined. Mechanisms of liquid-phase and gas-phase oxidative functionalization of carbon nanotubes with a conical and cylindrical form of graphene layers were proposed. Partial reaction rates were determined for carboxylation of carbon nanotubes. The thermal effects of liquid-phase and gas-phase oxidation of carbon nanotubes by nitric acid were estimated. The possibilities of secondary transformations of oxidized carbon nanotubes and the effects exhibited by functionalized forms when introduced into polymer matrices were shown. Using the experimental data, mathematical models of reactors for pilot-industrial realization of liquid-phase and gas-phase functionalization of carbon nanotubes were proposed. A draft process scheme for multi-batch production of functionalized forms of carbon nanotubes was developed.

Keywords

Carbon nanotubes; functionalization; mechanisms; modeling; thermal effects; technological realization.

Introduction

Nanostructures based on graphene planes represent a whole class of materials characterized by a variety of physicochemical properties [1, 2]. Their typical representatives are carbon nanotubes (**CNTs**), which are already being produced in fairly large quantities. They have broad application prospects as adsorbents [3–5], catalyst carriers [6, 7], electrode materials of supercapacitors and electrochemical current sources [8–12], as well as modifying additives in oils [13] and polymer composites with improved strength properties [14–16], high thermal and electrical conductivity [17, 18], and thermal stability [19–21].

To enhance the interaction of carbon nanotubes with polymer matrices and to minimize agglomeration phenomena, various methods of chemical surface treatment, leading to the formation of functional groups, are used. Through the functionalization of CNTs, it is possible to achieve much better results on the qualitative characteristics of composites [22–28] with reduced consumption rates, which significantly increases the economic effect of the application.

In this regard, the functionalized forms of CNTs are becoming more and more in demand on the market. At the same time, the supply of such forms is rather limited due to the fact that they are produced mainly in laboratory conditions. The methods used are often complex, multi-stage, and time-consuming, and require the use of expensive and highly toxic reagents [23, 27, 28].

The task of selecting the methods of chemical treatment of carbon nanomaterials available for industrialization is urgent. In this case, a detailed study of the regularities of CNT functionalization processes is a prerequisite for the formation of the basic principles of their scaling and optimization, as well as the development of technological schemes for the production of carbon nanomaterials of polyfunctional purpose.

In connection with this, the purpose of this study is to create physicochemical bases for the production of

functionalized forms of carbon nanomaterials, find the most important regularities in the interaction of carbon nanomaterials with oxidizing reagents and secondary transformations of oxidized forms for scaling these processes and predict the properties of products with varying regime parameters.

Materials and methods

The object of the study is CNTs synthesized on various catalytic systems by the CVD method [29] at OOO Nanotechcenter (Tambov, Russia). Their main parameters are presented in Table 1.

Carbon nanotubes underwent the following types of chemical treatment:

– oxidation with a mixture of equal volumes of a 30 % aqueous solution of hydrogen peroxide and 25 % aqueous ammonia. The CNTs were then ultrasonically distributed in NH_3 solution, and then a H_2O_2 solution was added to the resulting suspension. For 100 ml of a peroxide-ammonia mixture (50 ml of aqueous ammonia and 50 ml of hydrogen peroxide solution), 1 g of CNT was added. The reaction was carried out both at room temperature and with heating to 40–80 °C for 2–6 hours;

– mechanochemical oxidation of CNTs with a mixture of aqueous ammonia and ammonium persulfate pre-refined from the catalyst residues in a bead mill for 4–8 hours;

– oxidation with an acidified solution of potassium permanganate as in the procedure [30];

– liquid phase oxidation of nitrogen at a temperature of 40 to 120 °C and an acid concentration of 20 to 65 % for 0.5 to 24 hours;

– oxidation in hydrogen peroxide vapor at a temperature of 140 °C for 1–20 hours;

– oxidation in nitric acid vapor at a temperature of 120–180 °C for 1–8 hours;

– oxidation at room temperature by an ozone-air mixture (20 g of O_3 in 1 m^3 of air) in the absence and presence of an activating reagent (anhydrous nitric acid or sulfur trioxide formed by the evaporation of oleum);

– treatment of carboxylated carbon nanotubes with gaseous ammonia at 180–300 °C for 1–10 hours.

Changes in the structure and morphology of CNTs by treatment with various reagents were evaluated by X-ray diffraction analysis (DIFFRE-401), Raman spectroscopy (DXR Raman Microscope Thermo Scientific, excitation laser wavelength 532 nm), scanning (SEM) and translucent (TEM) electron microscopy (JOEL JEM-1011, JEM 2100, JEOL.JSM 6380LA). In order to establish the elemental composition of the samples, energy-dispersive analysis (JED 2300) was performed in parallel with SEM and TEM in a number of experiments. The specific surface area of CNTs was measured by the BET method for nitrogen adsorption at 77 K on a Nova 1200e Quantachrome device.

Qualitative and quantitative evaluation of the emerging surface groups in the covalent functionalization of CNM was carried out by means of X-ray photoelectron spectroscopy (XPS) spectroscopy (Kratos Axis Ultra DLD), infrared (IR) spectroscopy (Infraluum FT-801, wave range 4000–550 cm^{-1}), thermogravimetric (STA 449 F3 Jupiter Netzsch) and titrimetric analysis [31].

The analysis of gaseous products was carried out by means of gas chromatography on a Kristall-2000

Table 1

The main parameters of CNTs used in the work

Indicators	Type of CNT		
	Taunit	Taunit-MD	Taunit-M
Shape of graphene layers	conical	predominantly cylindrical	
Orientation of nanotubes	Chaotic	Beams + Chaotic	Chaotic
Catalyst	Ni/Mg	Fe/Co/Mg/Al	Co/Mo/Mg/Al
Outer diameter, nm	20–70	30–80	8–15
Inside diameter, nm	5–10	10–20	4–8
Length, μm	2 and above	20 and above	2 and above
Total amount of impurities (%) (after treatment)	up to 5 (up to 1)	3–4 (up to 1)	
Bulk density, g/cm ^{3}	0.4–0.6	0.03–0.05	
Specific geometric surface, m^2/g	120–130	180–200	300–320

instrument. The use of two packed columns (with CaA zeolite and polymeric sorbent "Chromosorb") made it possible to qualitatively and quantitatively identify CO, CO_2, N_2O, NO, NO_2, Ar, O_2 and N_2, which are present in the gas mixture at the exit from liquid-phase and gas-phase reactors after nitric acid oxidation of CNTs.

Results and discussion

Liquid-phase functionalization

The group of these functionalization methods is most often applied to carbon nanostructures. The methods presented in this paper were chosen basing on the simplicity of their implementation and the possibility of scaling.

However, as it turned out, not all of them are effective. In particular, it was shown that oxidation in the peroxide-ammonia system promotes the formation of hydroxyl groups on the surface of conical CNTs, which is confirmed by the appearance on the IR spectrum and the increase in the peak intensity at 3470 cm^{-1} (Fig. 1).

According to the Raman spectroscopy data (Table 2), processing in this system affects the defect index of the Taunit CNT, slightly lowering it. And this influence is strengthened as the duration and processing temperature increase. Consequently, oxidation of the Taunit CNT in this system "heals" the surface defects and / or removes the amorphous phase. However, this system does not have a similar effect on cylindrical Taunit-M and Taunit-MD CNTs, which is due to both a lower content of amorphous carbon in these materials and a smaller number of sp^3-carbon atoms in the surface layers of cylindrical CNTs.

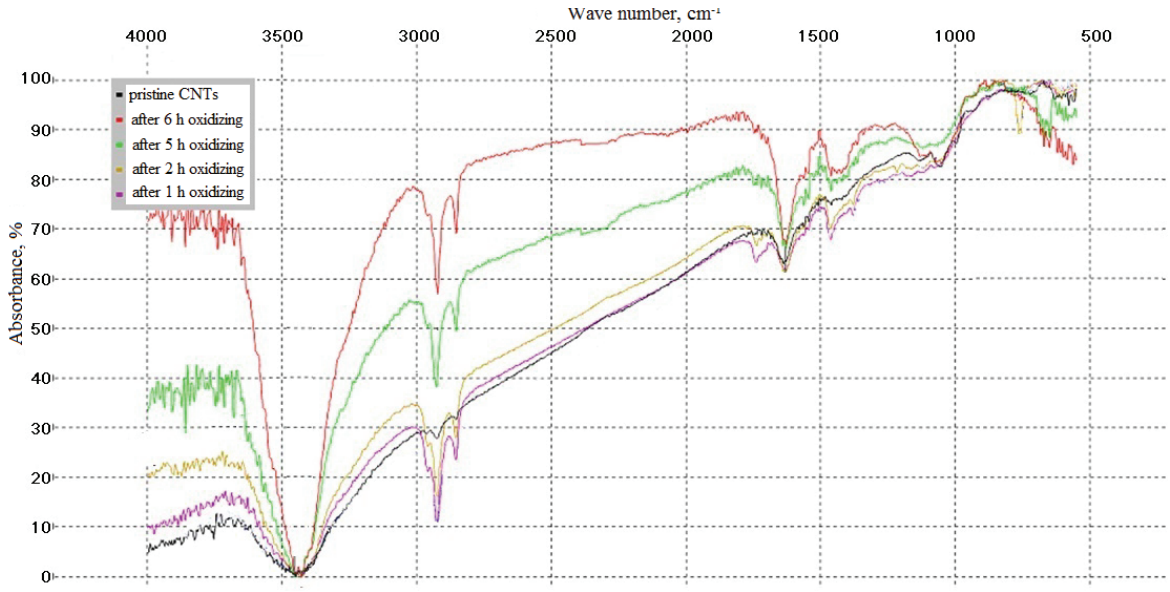

Fig. 1. IR spectra of raw Taunit CNTs and their modification during oxidation with $NH_4OH + H_2O_2$

Table 2

Change in the D/G indices calculated from the Raman spectra
(during the oxidation of CNTs in the peroxide-ammonia system)

Treatment conditions in the peroxide-ammonia system		Value D/G* for CNT		
Temperature, °C	Duration, h	Taunit	Taunit-M	Taunit-MD
Raw CNTs			0.79	0.45
20	6	0.92	0.80	0.46
40			0.78	0.45
60	4	0.87	0.79	
	6	0.78		0.46
80	2	0.80	0.78	
	4	0.74	0.76	0.47
	6	0.69		

* The values in the table are the means for 10 measurements (error ≤ 5 %).

The degree of functionalization (D_f) for all CNTs is very low (below the sensitivity threshold of titrimetry), which indicates the ineffectiveness of the application of the method with the aim of forming functional groups of acidic character.

Ammonium persulfate is an effective reagent for the oxidative functionalization of CNTs of various types in combination with mechanical processing in a bead mill. According to electron microscopy (Fig. 2), the nanotubes are shortened and deagglomerated, and on their surface, according to the data of X-ray photoelectron spectra, amine groups are formed in addition to hydroxyl and carbonyl groups, which contributes to the best compatibility with epoxy matrices.

The degree of functionalization of Taunit-M CNTs by carboxyl groups determined by the potentiometric reverse acid-base titration method is practically independent of the conditions of mechanochemical treatment and is 0.2–0.3 mmol/g (Table 3). The Raman spectra in the mechanooxidation of CNTs vary insignificantly.

This method of mechanochemical treatment of CNTs is protected by the RF patent [32]. It allows obtaining truncated functionalized carbon nanotubes, which have good dispersibility in water and polar organic solvents. The method can be easily scaled and relatively environmentally friendly.

Oxidation of CNT with potassium permanganate allows achieving higher values of the degree of functionalization (up to 1.5 mmol/g of COOH-groups, Fig. 3). Moreover, this parameter is easily regulated by the consumption of permanganate in relation to CNTs. The effect of the degree of functionalization of CNTs oxidized with potassium permanganate on the properties of polysulfone-based composites was found.

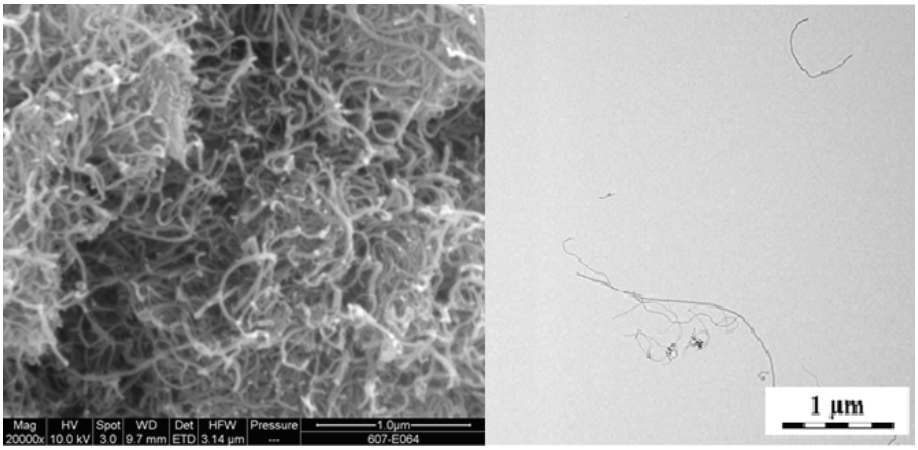

a) *b*)

Fig. 2. SEM (*a*) and TEM (*b*) images of mechanically oxidized Taunit-M CNT

Table 3

Properties of mechanically oxidized Taunit-M CNTs

Mechanical oxidation conditions		The value of the ratio of the intensities of the peaks on the Raman spectra for D/G	Degree of functionalization with carboxyl groups, mmol/g
The amount of ammonium persulfate consumed by 12 g of CNT, mole	Treatment duration, h		
0.1	4	1.01	0.20
0.2		1.05	0.26
0.2	8	1.09	0.28
0.3	4	1.11	0.30
Raw CNTs		1.04	–

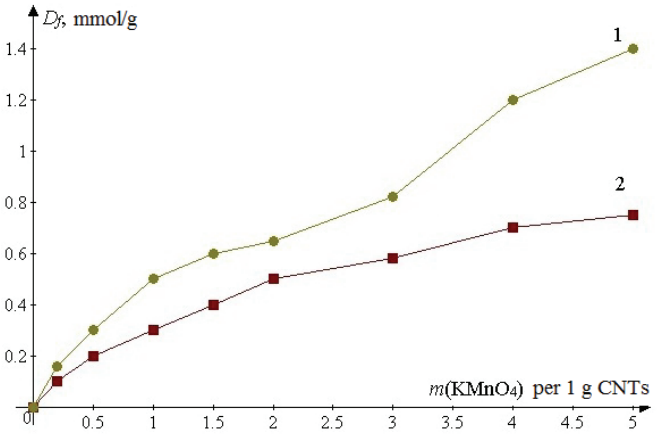

Fig. 3. Influence of oxidizer consumption (per unit mass of CNT) on the degree of functionalization of carboxyl compounds D_f for Taunit-M (*1*) and Taunit-MD (*2*) CNTs

It is shown that, despite the improvement in the dispersibility of CNTs (Fig. 4) with increasing D_f, the conductivity of composite films decreases. In connection with this, when oxidizing CNTs, it is important not only to promote the formation of a certain type of functional groups, but also to take into account their number.

In particular, one of the reasons for the decline in the quality of composites based on functionalized nanotubes is the possible destruction of surface layers (Fig. 5). For example, treatment with potassium permanganate for Taunit-M CNTs showed that with shallow oxidation it is possible to reduce the degree of defectiveness of CNTs by removing the amorphous phase during oxidation. However, starting from a certain moment, the degree of defectiveness of the material begins to increase. The search for oxidation conditions, in which destructive changes in CNTs are minimal, is an important task.

Oxidation with potassium permanganate is a fast, efficient laboratory method for the regulated functionalization of CNTs. However, the use of this method on an industrial scale is associated with a high consumption of potassium permanganate and limited resources, the toxicity of manganese salts and their unproductive losses (as part of the acidic filtrate that requires disposal).

The most suitable for scaling is the oxidation of CNTs with nitric acid because of its effectiveness with minimal destructive effect on graphene layers of CNTs. To study the technology of oxidation of CNTs with nitric acid, the regularities of this process on various types of CNTs were studied. At the initial stage, the qualitative and quantitative composition of the surface functional groups formed on different types of CNTs by oxidation with concentrated nitric acid was analyzed by the methods of IR spectroscopy, energy dispersion analysis (Table 4) and titrimetry (Fig. 6). It is shown that the nature of oxygen-containing groups does not depend on the shape of graphene layers of nanotubes. For all the types of CNTs studied, the values of D_f are characterized by functional groups in the following order: *carboxyl* > *phenolic* > *lactone*. Moreover, the behavior and properties of the material are determined by the content of the carboxyl groups.

The degree of functionalization of COOH groups depends on the type of oxidized CNTs. In the first hours of oxidation of Taunit CNTs are characterized by the highest value of D_f, which is due to the greater reactivity of conical layers and the presence of COOH groups in the starting material as a result of the characteristics of the production technology. However, then in terms of D_f, the CNTs are arranged in the following order (in ascending order): Taunit-MD – Taunit – Taunit-M. And, the difference is not so significant. The presented dependence shows the time intervals in which it is possible to obtain carboxylated CNTs of each type with a given value of the degree of functionalization.

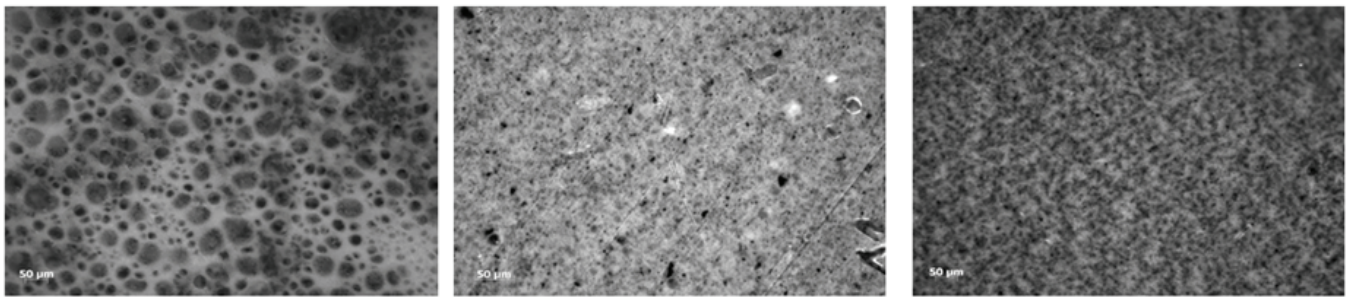

a) *b*) *c*)

Fig. 4. Photomicrographs of polysulfone films (Ultrason 6020 "Basf") modified by raw Taunit-M CNTs (*a*) and oxidized potassium permanganate (*b* and *c*) Taunit-M CNTs (D_f = 0.33 (*b*) and 0.90 (*c*) mmol/g)

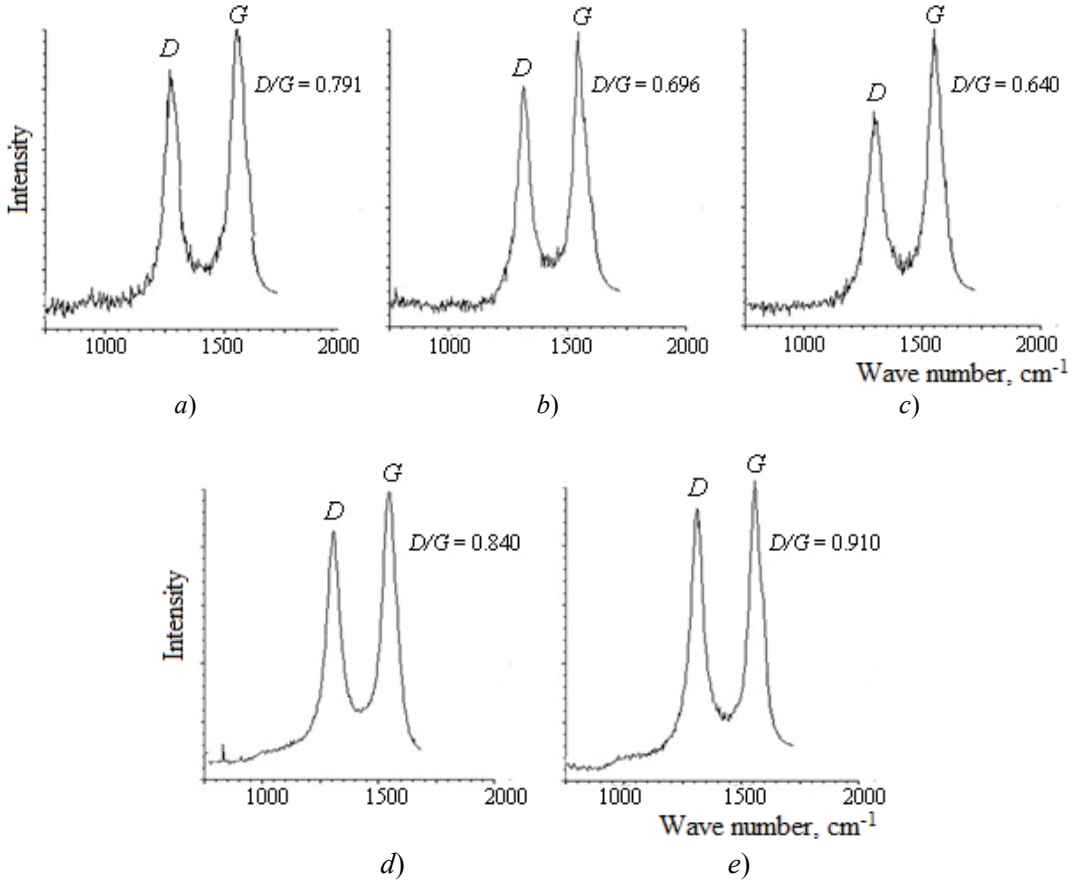

Fig. 5. Fragments of Raman spectra of raw Taunit-M CNTs (*a*) and oxidized by potassium permanganate Taunit-M CNTs at the ratio *m* ($KMnO_4$):
m (CNT), equal to 0.2 (*b*); 1.0 (*c*), 3.0 (*d*) and 4.0 (*e*)

Cylindrical Taunit-MD CNTs have the lowest values degrees of functionalization. The concentration of functional groups on the surface of the conical Taunit CNTs, close in geometric parameters to the Taunit-MD CNTs, is somewhat higher, since multiple sp^3-hybridized carbon atoms located on the protruding ends of their graphene layers, as well as carbon atoms with uncompensated valences, are more are more reactive than the sp^2-hybridized carbon atoms that make up the graphene surface of cylindrical nanotubes.

This is confirmed by transmission electron microscopy data (Fig. 7). The shape of graphene layers on the TEM image of the original Taunit CNTs is not clearly visible. However, even after a 2-hour oxidation in HNO_3, the destruction of the side walls of nanotubes begins, with defects evidently propagating along conical graphene layers, as a result of which their shape begins to be clearly seen. After an 8-hour treatment, changes in the morphology of the material are evident: individual nanotubes become thinner, break down into shorter fragments, and increase the content of the amorphous phase.

Table 4

Mass content of oxygen (%) in the raw and oxidized CNTs at 100 °C with concentrated nitric acid (c.p.)

CNT type	Mass fraction of oxygen in the samples according to the energy-dispersive analysis (%) for the oxidation time in HNO_3, h			
	0	2	8	10
Taunit	5.3	8.2	8.5	–
Taunit-M	0	4.2	11.8	14.4
Taunit-MD		–	6.1	6.6

After 3.5–4 hours of treatment, the highest degree of functionalization is characteristic of the Taunit-M CNTs, despite the fact that these are cylindrical nanotubes, which is due to their high specific surface area. According to the TEM data during oxidation of the Taunit-M CNTs in concentrated nitric acid, fractures and defects on individual nanotubes become larger, while their diameter and length do not practically change (Fig. 8).

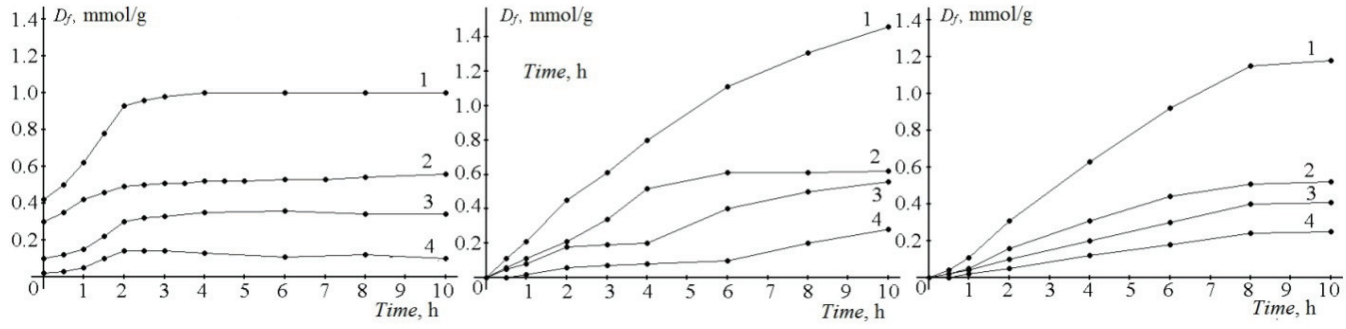

Fig. 6. Change in the total content of acid functional groups *1* and the degree of functionalization with carboxyl *2*, phenyl *3* and lactone *4* groups during oxidation with concentrated nitric acid of Taunit (*a*), Taunit-M (*b*) and Taunit-MD (*c*) at t = 100 °C

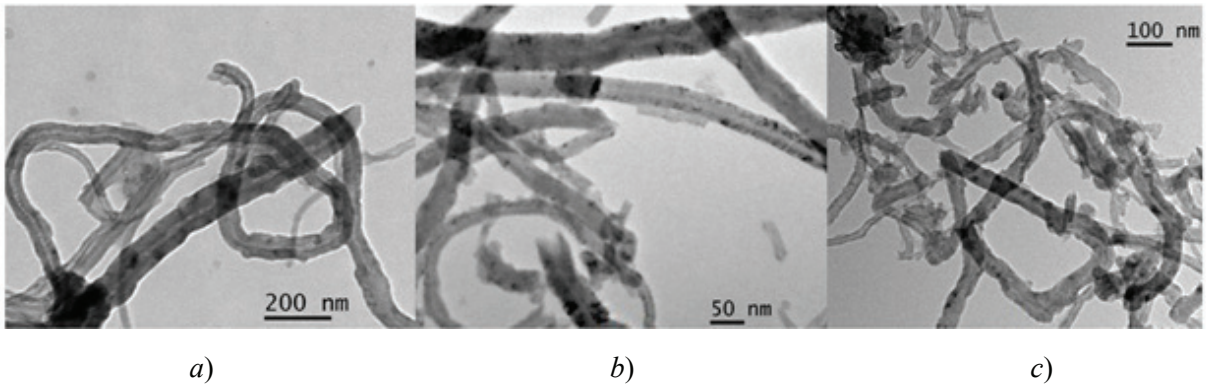

Fig. 7. TEM images of raw Taunit CNTs (*a*) and oxidized Taunit CNTs by concentrated nitric acid for 2 (*b*) and 8 (*c*) hours

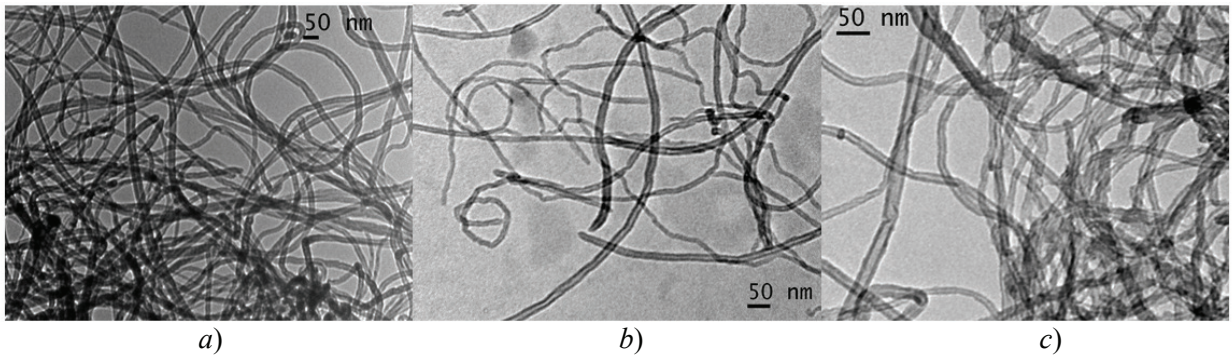

Fig. 8. TEM images of the raw Taunit-M CNTs (*a*) and the ones oxidized with concentrated nitric acid for 2 (*b*) and 8 (*c*) hours

The Raman spectroscopy data (Fig. 9) indicate a higher defectiveness of the raw Taunit-M CNTs. Consequently, the reactivity of these nanotubes is also related to the fact that more vacancies are present on their surface, which is more developed than that of the Taunit-MD CNTs. Also, the presence of an amorphous phase in the starting materials cannot be ruled out. Indeed, at the beginning of the oxidation process, a decrease in the D/G ratio for the Taunit-M CNTs is observed, which can be associated with intense oxidation and removal of the amorphous phase. But then the defectiveness index begins to grow, which is associated with a violation of the symmetry of graphene layers in the formation of functional groups.

In addition to the treatement time, the CNT oxidation rate and the achieved functionalization degree are influenced by factors such as the temperature of the reaction mass and the initial concentration of nitric acid therein. A typical form of the temperature dependence of D_f is shown in the diagrams of Fig. 10. They show that it is expedient to conduct the process at a temperature of 100–110 °C. In the case of Taunit-M and Taunit-MD CNTs, there is a clear tendency to increase the degree of

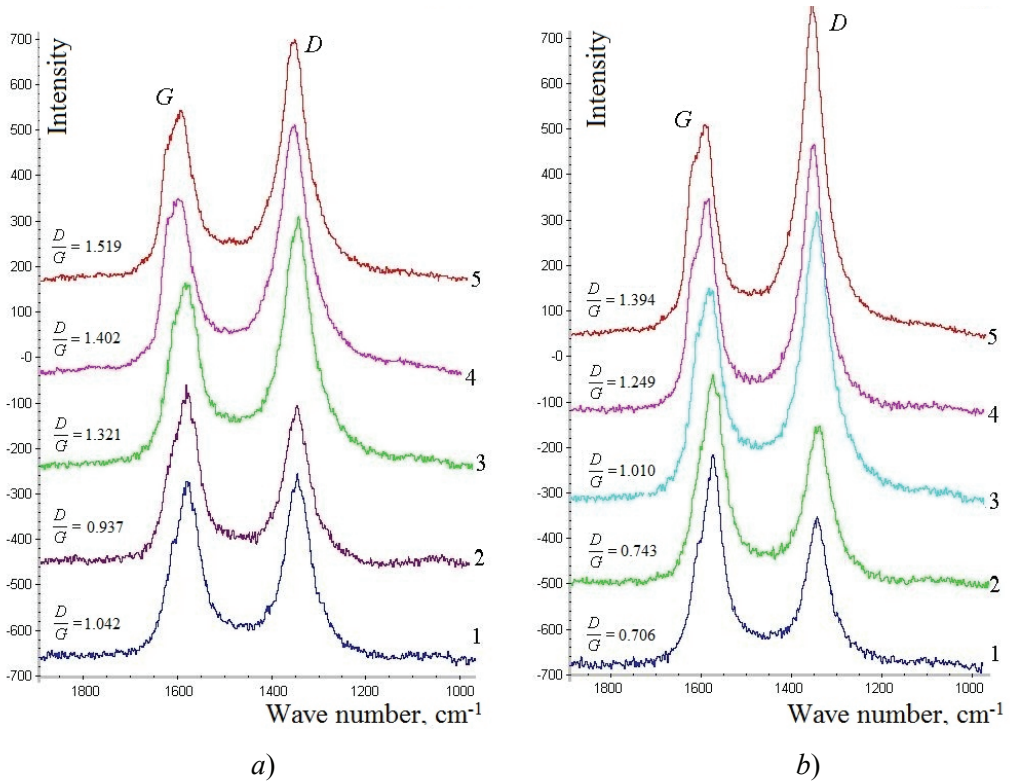

Fig. 9. The Raman spectra of the Taunit-M (*a*) and Taunit-MD CNTs (*b*):
raw (*1*) and oxidized by concentrated nitric acid during 1 (*2*); 3 (*3*); 4 (*4*) and 6 (*5*) hours

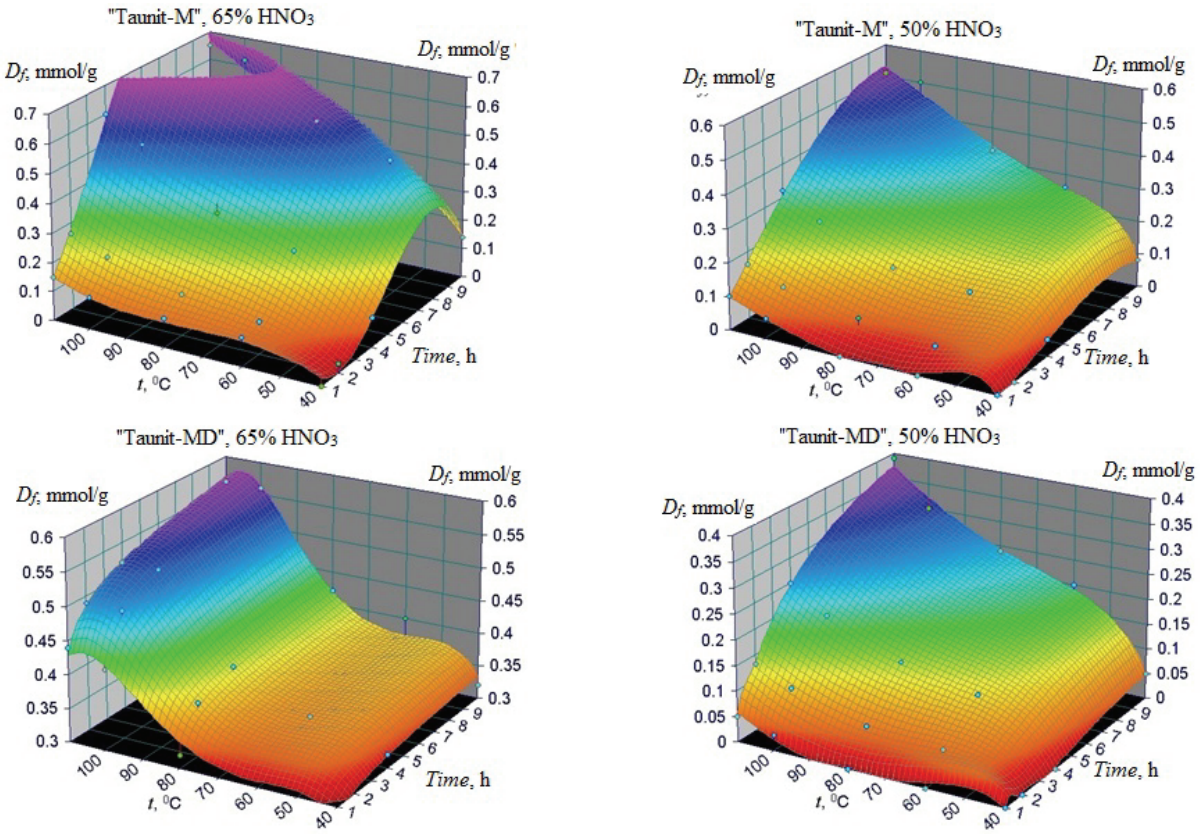

Fig. 10. The change in the degree of functionalization of CNTs by carboxyl groups D_f when oxidized with nitric acid in the "temperature-time" coordinates

functionalization at a higher temperature. However, taking into account that boiling of the reaction mass is possible at $t > 110$ °C, it is not necessary to raise the temperature above this interval. Underdevelopment of the reaction mass to boiling allows for a simpler instrumental design of the process. In addition, structural materials are unstable in boiling nitric acid.

Linearization of the obtained data in the coordinates of the Arrhenius equation made it possible to estimate the average effective activation energy of the process of CNT functionalization of various types (Table 5). These values suggest the course of the target reaction of the formation of functional groups in the region of mixed diffusion-kinetic control. The tendency to an increase in the fraction of diffusion limitations with increasing specific surface of CNTs is obvious. Moreover, the influence of this factor prevails over the influence of the degree of defectiveness of graphene layers on which the reactivity of the CNT surface depends.

The processing of data on the rate of formation of carboxyl groups by the equations of formal kinetics showed that the process is best described by the laws for first-order reactions on the surface of the Taunit-M and Taunit-MD CNTs. Moreover, for the Taunit-M CNTs in the coordinates of the first order, there are 2 linear sections, each of which is characterized by its own value of the effective rate constant (Fig. 11).

An explanation is the realization of a stage scheme in which the carboxyl groups are formed first at the ends and defects of the CNT side walls, and then on the fragments of the destroyed graphene layers formed as a result of the destruction [33]:

$$\text{CNTs} \overset{k_1}{\rightarrow} \text{CNTs–COOH} + \text{CNTs} = \text{O} + \text{CNTs–OH}\ldots \overset{k_2}{\rightarrow}$$

$$\overset{k_2}{\rightarrow} \text{CFs–COOH} + \text{CFs=O} + \text{CFs–OH}\ldots \overset{k_3}{\rightarrow} \text{CO}_2,$$

CNTs are carbon nanotubes; CFs are fragments of the side walls of CNTs.

The rate of the second stage is obviously higher than the first one. The confirmation of the possibility of this mechanism is that according to the Raman spectra,

Table 5

The values of the apparent activation energy (E_A^*) of the liquid phase carboxylation process of CNTs

CNT type	Taunit	Taunit -M	Taunit-MD
E_A^*, kJ/mol	37.0 ± 4.1	29.6 ± 3.2	21.9 ± 2.5

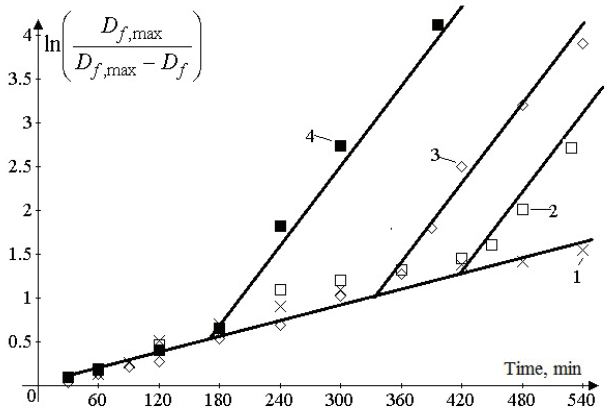

Fig. 11. Processing of kinetic data on the formation of carboxyl groups on surface of Taunit-M CNTs during liquid-phase oxidation in 30 (*1*); 40 (*2*) и 50 % (*3*) nitric acid at 100 °C in the coordinates of the first one

($D_{f,\max}$ is the limiting value of the degree of functionalization achieved under given conditions)

after a 3-hour oxidation of the Taunit-M CNTs, a pronounced increase in the defectiveness index *D/G* begins. The softening of oxidation conditions helps to slow down the destructive changes, therefore, a decrease in the concentration of nitric acid leads to an increase in the duration of the first section, until the disappearance of the second portion in the investigated time interval.

The Taunit-MD CNTs are more resistant to destruction of lateral walls due to initially less defectiveness. Apparently, therefore, on the dependence describing the kinetics of the formation of carboxyl groups on a given CNT type, there is one linear section in the first-order coordinates in the investigated time interval (Table 6).

The formation of carboxyl groups on the Taunit CNTs with conical graphene layers, in contrast to a similar process in the oxidation cylindrical nanotube satisfactorily described regularities formal kinetics for the second-order reaction that is caused by different character localization of functional groups, which are formed uniformly throughout the graphene layers of the surface. This is confirmed, among other things, by the nature of the destructive changes of the Taunit CNTs. Differences in the mechanisms of oxidation of different morphological types of CNTs that determine the empirical values of the kinetic parameters of the process, were confirmed in [34], where it was shown that the formation of the carboxyl groups occurs uniformly on the entire surface of the conical CNTs.

The effect of nitric acid concentration in time on the rate of formation of carboxyl groups on different types of CNTs is shown in the diagrams of Fig. 12. In connection with a significant decrease in the degree of functionalization of CNTs by carboxyl groups of all

types, even with a small decrease in the concentration HNO_3, it is advisable to use nitric acid with a concentration of at least 60 % for efficient process control. Also, the choice of concentrated nitric acid is due to the passivating effect on metals and alloys from which process equipment can be manufactured.

In view of the possible variations in the physicochemical parameters within a single type of CNT, the effect of incoming CNT parameters on the resulting indicators of the degree of functionalization and the change in the degree of defectiveness was shown (Table 7).

Table 6

Effective rate constants for the formation of carboxyl groups (k) in the oxidation of CNTs in concentrated nitric acid at 100 °C

Taunit-M CNT		Taunit-MD CNT		Taunit CNT	
Oxidation time, h	k, s^{-1}	Oxidation time, h	k, s^{-1}	Oxidation time, h	k, $g \cdot mol^{-1} \cdot s^{-1}$
0.5	$5.7 \cdot 10^{-5}$	1.0	$2.8 \cdot 10^{-5}$	1.0	$1.0 \cdot 10^{-3}$
1.0	$5.4 \cdot 10^{-5}$	2.0	$5.1 \cdot 10^{-5}$	2.0	$1.4 \cdot 10^{-3}$
2.0	$5.7 \cdot 10^{-5}$	3.0	$5.4 \cdot 10^{-5}$	2.5	$1.4 \cdot 10^{-3}$
3.0	$6.1 \cdot 10^{-5}$	3.5	$6.1 \cdot 10^{-5}$	3.0	$1.5 \cdot 10^{-3}$
4.0	$1.3 \cdot 10^{-4}$	4.0	$6.3 \cdot 10^{-5}$	4.0	$1.5 \cdot 10^{-3}$
5.0	$1.5 \cdot 10^{-4}$	5.0	$6.2 \cdot 10^{-5}$	5.0	$1.6 \cdot 10^{-3}$
6.0	$1.9 \cdot 10^{-4}$	5.5	$6.6 \cdot 10^{-5}$	6.0	$1.5 \cdot 10^{-3}$

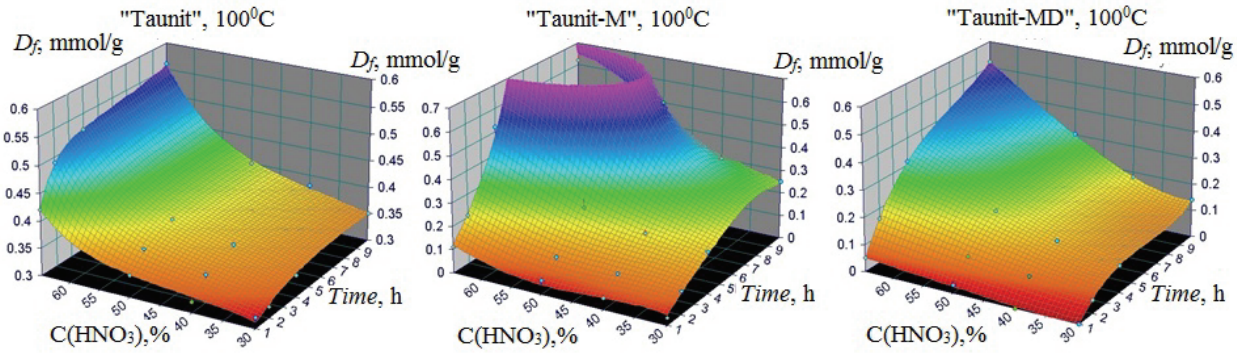

Fig. 12. The change in the degree of functionalization of CNTs by carboxyl groups D_f in the coordinates "concentration of HNO_3 – time"

Table 7

The most important characteristics of the raw and CNTs the ones oxidized with concentrated nitric acid (100 °C, 5 h)

CNT batch, No.	Raw CNT parameters					Oxidized CNT parameters		Increase in D/G after oxidation
	Bulk density*, kg/m^3	Collapse angle*, deg.	Angle of repose, deg.	Angle of tornado, deg. *	D/G***	D_f**, mol/g	D/G***	
1	9.85	12.33	46.33	34.00	0.756	0.7	1.221	1.62
2	13.40	13.00	43.00	30.00	0.845	0.8	1.322	1.56
3	11.90	15.67	42.00	26.33	0,880	0.9	1.309	1.49
4	22.40	16.67	45.00	28.33	0.988	1.0	1.163	1.18
5	12.75	14.00	42.67	28.67	1.099	1,2	1,322	1.20
6	16.30	20.00	45.33	25.33	1.159	1.3	1.325	1.14

* Measured on the VT-1000automated analyzer of powder materials.

** Determined titrimetrically.

*** Calculated from Raman spectra recorded on a DXR Raman Microscope (Termo Scientific) for λ = 532 nm.

The achievable value of D_f is determined by the ratio of D/G. Moreover, the dependence $D_f = f(D/G)$ is practically linear (Fig. 13). The defect index is more significantly increased when CNTs are oxidized with a lower initial D/G ratio. Therefore, the control of the initial characteristics of CNTs and the choice of their type is due, first and foremost, to the value of the degree of functionalization necessary for the intended application.

Additional information necessary for the development of process technology is obtained on the basis of an analysis of gaseous products of the interaction of CNT with nitric acid. The change in the total volume of evolved gases (after the condensation of water vapor) during the oxidation of CNT is shown in Fig. 14, and the composition – according to gas chromatographic analysis – is presented in Table 8.

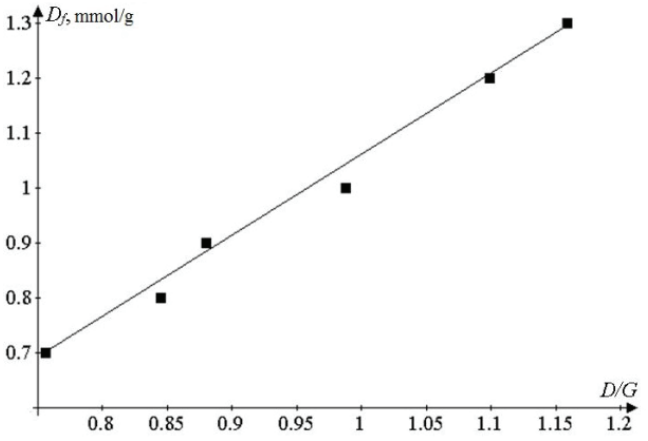

Fig. 13. Dependence of the degree of functionalization of CNTs with COOH groups after 5 hours of oxidation in 65 % nitric acid at 100 °C from the defect index D/G of the raw nanotubes

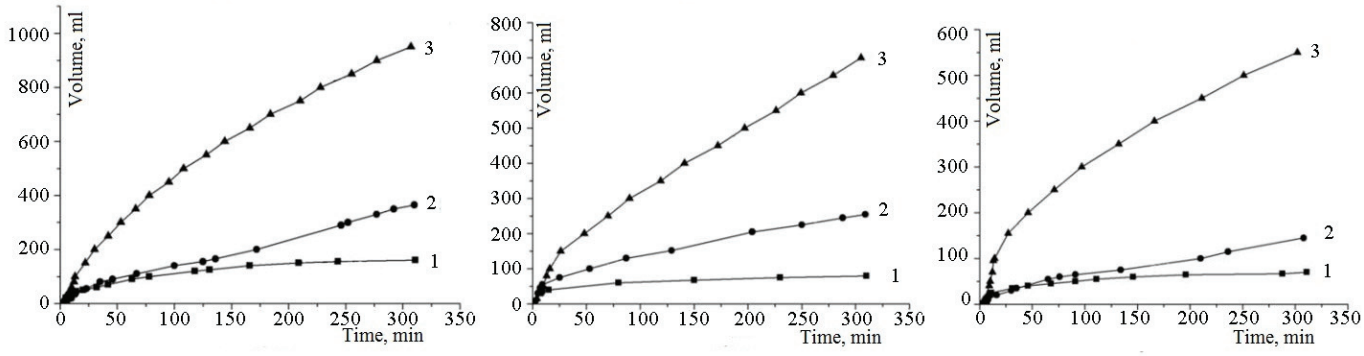

Fig. 14. The change in the total volume of released gases during the oxidation of Taunit-M (*a*), Taunit-MD (*b*) and Taunit CNTs (*c*) (in terms of 1 g of CNTs) with an initial nitric acid concentration equal to:
1 – 30 %; *2* – 40 %; *3* – 65 %; *t* = 100 °C

The most significant changes in the composition of reaction products occur at the initial stage. At this time, oxidation of any CNTs produces nitric oxide (I), but its proportion, as a rule, is no more than 1–2 % (vol.). According to the Raman spectra, at the same stage of the process, the residual amorphous phase is removed from the materials, on the basis of which it can be assumed that N_2O is formed during active oxidation.

The obtained results allowed making the necessary calculations for the organization of the stage of neutralization of waste gases during liquid-phase functionalization of CNTs. Also with their help and on the basis of [35–39], the most important chemical reactions that occur during the oxidation of CNTs by concentrated nitric acid were found:

$$C + 2HNO_3 = CO + 2NO_2 + H_2O; \quad (1)$$

$$C + 4HNO_3 = CO_2 + 4NO_2 + 2H_2O; \quad (2)$$

$$3C + 2NO_2 = 3CO + N_2O; \quad (3)$$

$$3C + 4NO_2 = 3CO_2 + 2N_2O; \quad (4)$$

$$C_n + 2HNO_3 = C_{n-1}–C(O) + 2NO_2 + H_2O; \quad (5)$$

$$2NO_2 + H_2O = HNO_2 + HNO_3. \quad (6)$$

In the reactions (1)–(2), both CNTs themselves and the amorphous phase inclusions can participate. In reactions (3)–(4), presumably, amorphous carbon is oxidized, since N2O is identified in the gaseous products only at the initial stage of the process. Moreover, its content is higher in gaseous oxidation products of the more defective Taunit-M CNTs. Equation (5) is a diagram of the formation of oxygen-containing functional groups on the surface of CNTs, which are generally designated as C(O).

Table 8

The composition of gaseous oxidation products of CNT with nitric acid
(according to gas chromatographic analysis)

CNT type	Time, min	The proportion of the component in the gas mixture, vol. %			
		CO	CO_2	N_2O	NO_2
Taunit	35	34.8	34.7	0.8	29.7
	85	24.7	38.0	1.0	36.3
	135	21.7	36.9		41.4
	185	16.3	37.1		46.6
	235	14.8	36.5		48.7
	285	12.6	41.5	–	45.9
	335	9.1	30.8		60.1
	385	8.5	31.7		59.8
	435	3.8	29.9		66.3
Taunit-M	20	3.8	25.3	0.7	70.2
	105	15.5	33.3	0.9	50.4
	155	17.8	32.1	1.9	48.1
	205	13.8	38.8		47.4
	255	13.4	37.0		49.6
	305	12.2	41.3	–	46.5
	355	12,9	37,2		49,9
	405	11.2	41.3		463
Taunit-MD	35	53.4	31.6	0.5	14.5
	85	35.3	32.4		32.3
	135	28.2	37.1		34.7
	185	26.4	36.8	–	36.8
	235	24.8	36.1		39.1
	285	18.4	37.6		44.0
	385	15.2	36.0		48.8

Information on the total volume, qualitative and quantitative composition of the gases released during the oxidation of CNTs with concentrated nitric acid was used as initial data for estimating reaction rates (1)–(2) and (5)–(6) (Table 9). The reaction rates (3)–(4) were not evaluated because of their negligible values, as indicated by the extremely low content of the product of these reactions - nitric oxide (I) in the gas composition.

The results obtained show that the actual functionalization of CNTs described by means of Eq. (5) is a reaction that makes the minimum contribution to the total process. The statement about the lower rate of functionalization of the Taunit-MD CNTs compared to the Taunit-M CNTs is fair.

The data of the carried out experimental researches are a basis for development of technologies of obtaining functionalized forms. The first stage was the thermal calculation of reactors based on the application of the balance equation:

$$Q_t + Q_r + Q_c + Q_h + Q_d + Q_m + Q_f = 0,$$

where Q_t is the amount of heat supplied from heating devices; Q_r is the amount of heat determined by the total thermal effect of chemical reactions; Q_c is the amount of heat determined by the change in the concentration of the components of the solution; Q_h is the amount of heat expended on heating the reactants and the structural elements that contact them; Q_d is the amount of heat dissipated in the form of heat losses to the environment; Q_m is the amount of heat introduced by the agitator; Q_f is the amount of heat corresponding to the heat of the phase transitions.

The non-stationary temperature field of a heat-insulated reactor body of liquid-phase functionalization with electric heating can be modeled by solving the heat conduction problem for a hollow unlimited cylinder with a functionally distributed heat source:

$$\frac{\partial t_b(r,\tau)}{\partial \tau} = a\left(\frac{\partial^2 t_b(r,\tau)}{\partial r^2} + \frac{1}{r}\frac{\partial t_b(r,\tau)}{\partial r}\right) + \frac{q(r)}{c\rho},$$

$$R_0 \le r \le R_1, \tau > 0; \qquad t_b(r,0) = f(r);$$

$$\lambda \frac{\partial t_b(R_0,\tau)}{\partial r} - \alpha_t\left(t_b(R_0,\tau) - t_r\right) = 0;$$

$$\frac{\partial t_b(R_1,\tau)}{\partial r} = 0.$$

Here $t_b(r, \tau)$ is temperature field in the heat-insulated wall of the apparatus with electric heating, °C as a function of the radial coordinate r, m, and time τ, s; a is thermal diffusivity of the wall material of the apparatus, m^2/s; $q(r)$ is power of a volumetric heat source, W/m^3; $f(r)$ is initial temperature distribution, °C; R_0, R_1 are internal and external radii of the wall of the apparatus with an electric heating device, m; λ is thermal conductivity of the wall material of the apparatus, W/(m·°C); α_t is coefficient of heat transfer from the apparatus wall to the reagents, $W/(m^2 \cdot °C)$; t_r is reagent temperature, °C.

Calculations for this model have made it possible to determine the parameters of the main equipment for performing liquid-phase oxidative functionalization of CNTs, ensuring a rational temperature regime of the process.

Table 9

The calculated amounts of gaseous products from the interaction of CNTs with concentrated nitric acid and the values of the rates (W_i) of the reactions

Type of CNT	Time, min	The amount of gaseous product formed during the oxidation of 1 g of CNT, mmol				The reaction rate, mol/(g·min)			
		CO_2	CO	NO_2	N_2O	W_1	W_2	W_5	W_6
Taunit	35	2.49	2.49	2.13	0.06	$7.12\cdot10^{-5}$	$7.11\cdot10^{-5}$	$3.90\cdot10^{-8}$	$1.76\cdot10^{-4}$
	85	4.21	3.61	3.78		$2.24\cdot10^{-5}$	$3.45\cdot10^{-5}$	$5.74\cdot10^{-9}$	$7.13\cdot10^{-5}$
	135	5.43	4.33	5.14		$1.43\cdot10^{-5}$	$2.43\cdot10^{-5}$	$2.28\cdot10^{-9}$	$4.93\cdot10^{-5}$
	185	6.44	4..77	6.41		$8.88\cdot10^{-6}$	$2.02\cdot10^{-5}$	$1.77\cdot10^{-9}$	$3.66\cdot10^{-5}$
	235	7.30	5.12	7.56	0.10	$7.70\cdot10^{-6}$	$1.73\cdot10^{-5}$	$1.27\cdot10^{-9}$	$3.01\cdot10^{-5}$
	285	8.19	5.39	8.54		$5.37\cdot10^{-6}$	$1.77\cdot10^{-5}$	$9.75\cdot10^{-10}$	$3.10\cdot10^{-5}$
	335	8.79	5.57	9.72		$3.56\cdot10^{-6}$	$1.20\cdot10^{-5}$	$7.81\cdot10^{-10}$	$1.59\cdot10^{-5}$
	385	9.36	5.72	1.08		$3.08\cdot10^{-6}$	$1.15\cdot10^{-5}$	$6.46\cdot10^{-10}$	$1.52\cdot10^{-5}$
	435	9.87	5.79	1.19		$1.29\cdot10^{-6}$	$1.01\cdot10^{-5}$	$5.47\cdot10^{-10}$	$1.03\cdot10^{-5}$
Taunit-M	20	1.58	0.24	4.40	0.04	$1.19\cdot10^{-5}$	$7.93\cdot10^{-5}$	$3.26\cdot10^{-8}$	$1.03\cdot10^{-4}$
	105	5.91	2.25	10.95	0.16	$2.37\cdot10^{-5}$	$5.09\cdot10^{-5}$	$2.95\cdot10^{-8}$	$1.63\cdot10^{-4}$
	155	7.50	3.13	13.33		$1.76\cdot10^{-5}$	$3.18\cdot10^{-5}$	$2.54\cdot10^{-8}$	$9.99\cdot10^{-5}$
	205	9.13	3.71	15.32		$1.16\cdot10^{-5}$	$3.26\cdot10^{-5}$	$2.24\cdot10^{-8}$	$1.13\cdot10^{-4}$
	255	10.51	4.21	17.17	0.25	$9.95\cdot10^{-6}$	$2.74\cdot10^{-5}$	$1.94\cdot10^{-8}$	$9.31\cdot10^{-5}$
	305	11.90	4.62	18.73		$8.21\cdot10^{-6}$	$2.78\cdot10^{-5}$	$1.63\cdot10^{-8}$	$9.63\cdot10^{-5}$
	355	13.05	5.02	20.28		$7.99\cdot10^{-6}$	$2.31\cdot10^{-5}$	$1.34\cdot10^{-8}$	$7.73\cdot10^{-5}$
	405	14.24	5.36	21.62		$6.47\cdot10^{-6}$	$2.38\cdot10^{-5}$	$1.03\cdot10^{-8}$	$8.16\cdot10^{-5}$
Taunit-MD	35	1.73	2.92	0.79		$8.33\cdot10^{-5}$	$4.93\cdot10^{-5}$	$8.41\cdot10^{-8}$	$3.35\cdot10^{-4}$
	85	3.24	4.57	2.30		$3.30\cdot10^{-5}$	$3.02\cdot10^{-5}$	$8.91\cdot10^{-9}$	$1.57\cdot10^{-4}$
	135	4.77	5.73	3.73		$2.33\cdot10^{-5}$	$3.06\cdot10^{-5}$	$4.02\cdot10^{-9}$	$1.40\cdot10^{-4}$
	185	6.20	6.75	5.16	0.03	$2.04\cdot10^{-5}$	$2.85\cdot10^{-5}$	$2.46\cdot10^{-9}$	$1.26\cdot10^{-4}$
	235	7.54	7.67	6.61		$1.84\cdot10^{-5}$	$2.68\cdot10^{-5}$	$1.72\cdot10^{-9}$	$1.15\cdot10^{-4}$
	285	8.90	8.34	8.20		$1.33\cdot10^{-5}$	$2.72\cdot10^{-5}$	$1.30\cdot10^{-9}$	$1.03\cdot10^{-4}$
	385	11.42	9.40	11.16		$1.06\cdot10^{-5}$	$2.52\cdot10^{-5}$	$9.32\cdot10^{-10}$	$8.79\cdot10^{-5}$

Gas-phase functionalization

CNTs that have undergone liquid-phase oxidation with nitric acid can be used in composites based on polar polymer matrices, and can also be a semi-product for subsequent (secondary) transformations. However, this method is not acceptable when it is necessary to preserve the bulk morphology of materials or particles of the metal oxide catalyst in the composition of oxidized CNTs. To achieve the necessary result in this case gas-phase oxidation of CNTs will allow. It was proposed to use hydrogen peroxide vapor at a temperature of 140 °C as an innovative method for the functionalization of CNTs as it has low production costs and high environmental friendliness.

This method of CNT treatment allows achieving a number of effects. Thus, by the Raman method, it was found that with a 10-hour oxidation in hydrogen peroxide vapor, the D/G index decreased for the Taunit-M CNTs, and then it began to grow. For the Taunit-MD CNTs from the very beginning of the process an increase in the degree of defectiveness was observed (Table 10). Similar dependences of the defectiveness index on the duration of oxidative treatment were revealed for CNTs of these types when oxidized with concentrated nitric acid. However, when

functionalizing in hydrogen peroxide vapor, destructive changes in CNTs were less significant for the Taunit-MD and Taunit-M CNTs, and in the case of the latter, a longer duration of "healing" of defects was observed.

According to the data of the XPS-spectra of CNTs treated in this system (Fig. 15), the oxygen content in the samples is small (up to 0.82 at. %), and it is part of the hydroxyl groups. Due to the low degree of functionalization, CNTs treated in hydrogen peroxide vapor do not form uniform dispersions in polar matrices. However, there is a structuring effect of CNTs functionalized by this method on composites based on synthetic rubber, epoxy resin and polysulfone, resulting in a noticeable improvement in radio-shielding and electrically conductive properties [40], which determines the field of practical application.

As methods that allow a large number of functional groups to be grafted onto the CNT surface while maintaining the volume-morphological characteristics, it has been proposed to oxidize with ozone and vapors of nitric acid. Treatment of CNT with an ozone-air mixture (1 vol. % O_3) at room temperature is effective only in the presence of vapors of anhydrous nitric acid or sulfur oxide (VI). To achieve high values of D_f during processing in this system, preliminary purification of CNT from impurities of metal oxide catalysts is necessary. These factors complicate the scaling of the process of ozone treatment of CNTs.

Treatment of CNTs in nitric acid vapor is possible without purification from catalyst impurities and contributes to the formation of 2–3 times more functional groups than in liquid-phase oxidation. According to the data of XPS-spectra, oxygen and nitrogen are present in the composition of CNT samples treated in vapors of nitric acid (Table 11). The latter is due to chemisorption on the CNT surface of nitrogen dioxide, which is the product of the thermal decomposition of HNO_3 under process conditions. The greatest content of oxygen is typical of CNTs unrefined from the catalyst, subjected to oxidation in this system.

The oxidized Taunit-MD CNTs are less defective than Taunit-M CNTs, which is illustrated by the large content of carbon atoms in the sp^2-state (Table 12). These data agree well with the results of Raman spectroscopy of the initial samples. The maximum amount of carboxyl groups is formed on the surface of the untreated Taunit-M CNTs. The removal of the metal oxide catalyst helps to reduce the degree of functionalization with COOH groups. The amount of carbonyl and phenolic groups becomes somewhat higher. Consequently, the particles of transition metal oxides catalyze the deep oxidation of CNTs.

Table 10

Assessment of the degree of defectiveness of the raw CNTs and the ones oxidized in hydrogen peroxide vapor at 140 °C from the data of the Raman spectra

CNT type	The value of the ratio *D/G* on the Raman spectra with the duration of oxidation, h				
	2	5	10	20	30
Taunit-M (raw)	0.930	0.781	0.728	0.854	0.938
Taunit-M (refined)	0.938	0.801	0.786	0.896	0.959
Taunit-MD (raw)	0.745	0.780	0.806	0.894	0.912

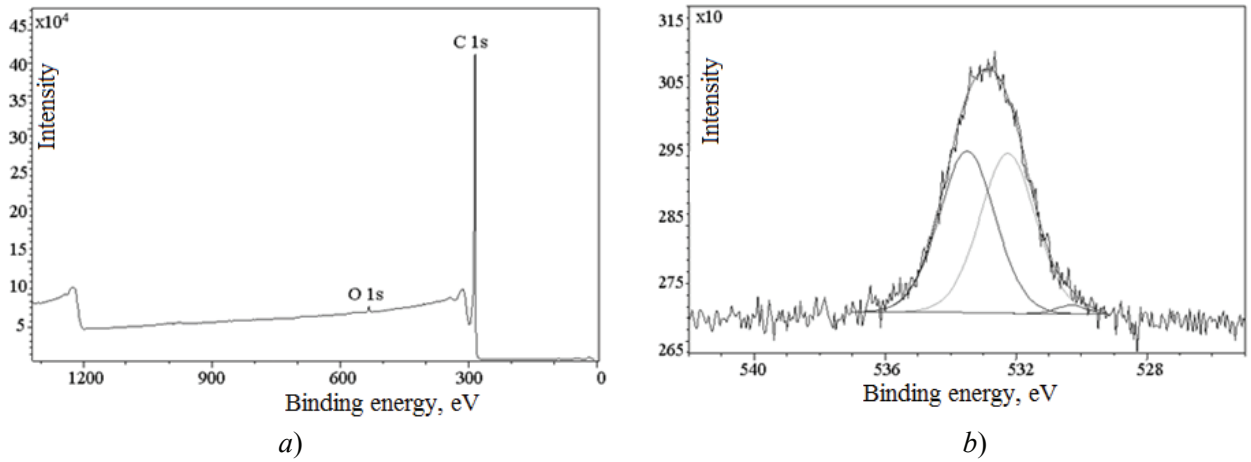

a) *b*)

Fig. 15. Panoramic XPS spectra (*a*) and XPS spectra to the photoelectron oxygen lines (*b*) of the pre-refined Taunit-M CNTs treated in hydrogen peroxide vapor at 140 °C for 20 hours

Table 11

Elemental analysis of CNT samples oxidized in nitric acid vapor at 140 °C for 6 hours, according to the XPS-spectra data

Type of oxidized CNTs	Element fraction, at. %		
	C	O	N
Taunit-MD (raw)	92.94	6.36	0.70
Taunit-M (treated)	93.31	5.88	0.81
Taunit-M (treated)	94.60	4.98	0.42

Table 12

The fraction of states of carbon atoms in C1s XPS-spectra of CNT samples oxidized in nitric acid vapor at 140° for 6 hours

Type of oxidized CNTs	Share of states, at. %				
	284.4–284.2 C–C (sp^2)	285.0–285.1 C–C (sp^3)	286.2–286.6 C–O	287.4–287.4 C=O, O–C–O	288.3–288.9 O=C–O
Taunit-MD (raw)	97.07	0.59	0.96	0	1.38
Taunit-M (raw)	94.98	2.23	0.96	0	1.83
Taunit-M (treated)	94.25	2.63	1.66	0.20	1.26

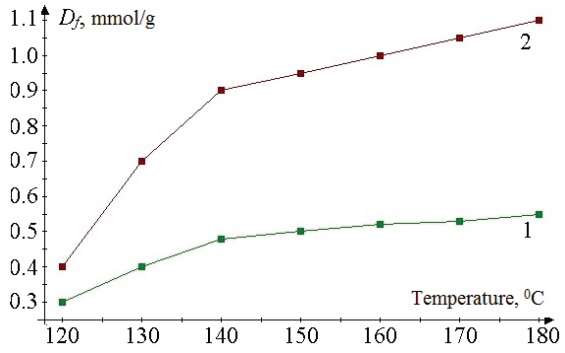

Fig. 16. Dependence of the degree of functionalization with COOH groups of the Taunit-M CNTs oxidized for 2 h (*1*) and 5 h (*2*) on the processing temperature in nitric acid vapor

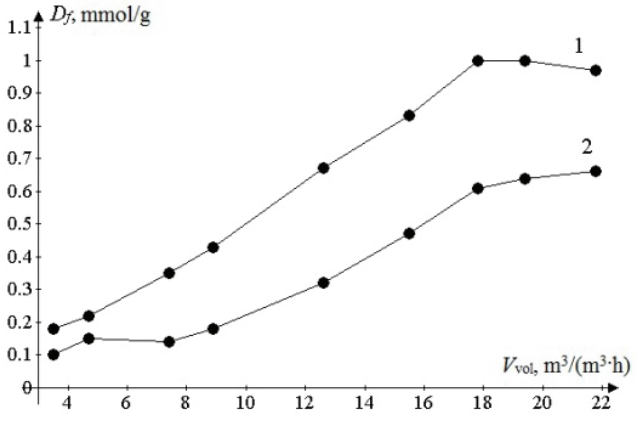

Fig. 17. Dependence of the degree of functionalization of the surface of the Taunit-MD CNTs on the volumetric feed rate of the reagent for 5-hour oxidation at 140 °C in nitric acid vapor

The degree of functionalization of CNTs in this case is determined by such factors as the temperature and duration of the process, the concentration and the rate of supply of the reactant vapor. The most pronounced growth of D_f is observed in the temperature range up to 140 °C (Fig. 16). A further increase in temperature has little effect on the efficiency of the process. Perhaps this is due to an increase in the rate of simultaneous de-functionalization of CNTs with the formation of carbon oxides. Moreover, despite the increase in the total oxidation rate, the degree of functionalization of CNTs can increase insignificantly, do not change or even decrease, which is confirmed by data on the change in the mass of CNT samples during oxidation in nitric acid vapor. Moreover, as the temperature of the process increases, the mass loss of the samples becomes more and more significant.

Increase in the volume flow rate of the reagent (V_{vol}) to 17.8 $m^3/(m^3 \cdot h)$ promotes an increase in the degree of functionalization, while maintaining the mass loss factor of the samples at the level of 10–12 %, after which, with a noticeable gain, the value of D_f ceases to increase (Fig. 17).

When using an oxidizing mixture diluted with argon (in a ratio of 1 : 5), the degree of functionalization practically ceases to depend on temperature. Moreover, it is also not possible to significantly reduce the mass loss of samples at temperatures 160–180 °C due to a decrease in the oxidant concentration (Table 13).

Table 13

Degree of functionalization of Taunit-M CNTs by carboxyl groups (D_f) and mass loss of samples after a 2-hour oxidation by dilute argon with nitric acid vapor

Temperature, °C	120	140	160	180
D_f, mmol/g	0.31	0.29	0.24	0.21
Average decrease in sample weight, % of initial	5.4	7.8	15.4	19.0

Thus, the gas-phase functionalization of CNTs in nitric acid vapor is expedient at temperatures of 140–150 °C.

Among other factors affecting the speed of the process, mention should be made of the presence of impurities of metal oxide catalysts and the morphological features of CNTs. Their allowance made it possible to determine rational treatment regimes in nitric acid vapor of the initial and refined CNTs of various types.

The processing of the obtained experimental data shows that oxidation in nitric acid vapor, regardless of the type of CNT, is satisfactorily described by the equations of formal kinetics of the first order. The calculated values of effective rate constants for the formation of carboxyl groups (k) are presented in Table 14. Unlike the liquid-phase process, there was no significant change in the value of k for the Taunit-M CNTs during the process, in spite of the rather high values of the achieved degrees of functionalization.

The values of the rate constants for different types of CNTs are relatively close. These facts indicate that the mechanisms of formation of functional groups in the gas-phase and liquid-phase oxidation of CNTs have pronounced differences.

The composition of gaseous products of CNT interaction with nitric acid vapor after condensation of water vapor includes oxides of nitrogen and carbon (Table 15).

In most sources dealing with the interaction of carbon materials with nitrogen oxides, it is noted that the first stage of the process is adsorption, which can be both physical and chemical. During chemisorption on the carbon surface, groups of composition –C–ONO, –C–ONO_2 or –C–NO_2, are formed; their transformations lead to the formation of carbon oxides, functional groups and products of reduction of nitrogen dioxide.

It was shown in [41–44] that when nitrogen dioxide is reduced, nitric oxide (II) is predominantly formed. The absence of this component in the gaseous products of CNT oxidation can be explained by the fact that NO is rapidly oxidized by oxygen produced by thermal decomposition of nitric acid ($4HNO_3 \rightarrow \rightarrow 4NO_2 + 2H_2O + O_2$). The absence of molecular nitrogen in products of the interaction of carbon with nitrogen oxides is indicated in [45]. In [46] it is noted that in addition to NO in the products of oxidation of carbon materials with nitrogen dioxide, N_2O is identified.

Thus, the information obtained on the composition of gaseous products of CNT oxidation in nitric acid vapor does not contradict the literature data. Consequently, the chemistry of oxidation of the CNT surface by the thermal decomposition products of HNO_3 is similar to the chemistry of oxidation of soot and graphite and can be described by a set of typical reaction equations. The most important of these are:

a) processes of formation of oxygen-containing functional groups:

$$C_n + NO_2 \rightarrow C_{n-1}C(O) + NO; \quad (7)$$

$$C_n + 1/2O_2 \rightarrow C_{n-1}C(O); \quad (8)$$

b) processes of formation and transformation of nitrogen-containing surface formations:

$$C + NO_2 \rightarrow C(NO_2); \quad (9)$$

Table 14

Effective rate constants for the formation of COOH groups k during the oxidation of CNTs in nitric acid vapor at 140 °C

Taunit-M		Taunit-MD		Taunit	
Time, h	k, s^{-1}	Time, h	k, s^{-1}	Time, h	k, s^{-1}
2.0	$3.3 \cdot 10^{-5}$	2.0	$4.4 \cdot 10^{-5}$	2.0	$1.0 \cdot 10^{-4}$
3.0	$2.7 \cdot 10^{-5}$	3.0	$4.7 \cdot 10^{-5}$	5.0	$5.4 \cdot 10^{-5}$
4.5	$2.5 \cdot 10^{-5}$	5.5	$5.1 \cdot 10^{-5}$	6.0	$3.2 \cdot 10^{-5}$
6.0	$2.8 \cdot 10^{-5}$	6.0	$5.5 \cdot 10^{-5}$	10.0	$3.2 \cdot 10^{-5}$

Table 15

Volume and composition of gaseous oxidation products 1 g of CNT in nitric acid vapor (V_{vol} = 17.8 $m^3/(m^3 \cdot h)$) at 140 °C according to the gas chromatographic analysis

Type of CNT	Time, h	The total volume of gaseous products after condensation of water vapor (normal conditions), l	The proportion of the component in the gas mixture, vol. %			
			CO	CO_2	N_2O	NO_2
Taunit-MD unrefined from catalyst impurities	1.5	0.83	5.3	17.2	0	77.5
	2.5	1.42	6.1	17.9	0.3	75.7
	3.5	1.93	5.1	16.1	0.7	77.0
	4.5	2.52	5.2	16.5	1.3	78.1
Taunit-M unrefined from catalyst impurities	1.5	0.78	12.2	5.3	0	82.5
	2.5	1.51	6.8	21.5	0.5	71.2
	3.5	2.01	6.8	17.7	0.6	74.9
	4.5	2.53	6.0	16.7	0.5	76.8
	6.0	3.17	5.1	13.6	0.9	80.4
Taunit-M refined from catalyst impurities	2.5	1.43	6.1	17.1	1.7	75.1
	3.5	1.95	5.7	15.8	1.2	77.3
	4.5	2.51	5.5	15.7	1.4	77.4
	6.0	3.11	4.8	12.8	0.9	81.5

$$C_{n-1}C(O) + NO_2 \rightarrow C_{n-1}C(ONO_2); \quad (10)$$

$$C_{n-1}C(ONO_2) \rightarrow C_{n-1} + CO_2 + NO; \quad (11)$$

$$C_{n-1}C(ONO_2) \rightarrow C_{n-1} + CO + NO_2; \quad (12)$$

c) processes of elimination of oxygen-containing functional groups:

$$C_{n-1}C(O) + NO_2 \rightarrow C_{n-1} + CO_2 + NO; \quad (13)$$

$$C_{n-1}C(O) + 1/2O_2 \rightarrow C_{n-1} + CO_2; \quad (14)$$

$$C_{n-1}C(O) + 2NO \rightarrow C_{n-1} + CO_2 + N_2O; \quad (15)$$

$$C_{n-1}C(O) \rightarrow C_{n-1} + CO; \quad (16)$$

d) processes of amorphous phase oxidation:

$$3C + 2NO_2 = 3CO + N_2O; \quad (17)$$

$$3C + 4NO_2 = 3CO_2 + 2N_2O; \quad (18)$$

$$C + NO_2 = CO + NO; \quad (19)$$

$$C + 2NO_2 = CO_2 + 2NO; \quad (20)$$

$$C + 2NO = CO + N_2O; \quad (21)$$

$$C + O_2 \rightarrow CO_2; \quad (22)$$

$$2C + O_2 \rightarrow 2CO; \quad (23)$$

$$C + CO_2 \rightarrow 2CO; \quad (24)$$

e) associated processes of interaction between reaction products:

$$2NO + O_2 = 2NO_2; \quad (25)$$

$$CO + NO_2 \Leftrightarrow CO_2 + NO; \quad (26)$$

$$2CO + O_2 = 2CO_2. \quad (27)$$

The water vapor that is present in the oxidizing mixture, as shown in [37, 47], catalyzes oxidation without changing the interaction mechanisms. According to the authors of [47], the catalytic effect is associated with the formation of nitric and acid nitrogen by reactions:

$$2NO_2 + H_2O = HNO_2 + HNO_3; \quad (28)$$

$$3HNO_2 = HNO_3 + 2NO + H_2O. \quad (29)$$

These acids can participate in the direct formation of intermediate complexes C–NO_2.

According to the data of Table 15, the total volumes of released gases at equal intervals do not depend on the type of oxidized CNTs, but are determined by the rate of supply of the oxidizing reagent.

The predominant component of the analyzed mixtures of gaseous products is NO_2. Its concentration during the process does not depend on the type of oxidized CNTs and practically does not change.

It ranges from 71.2 to 81.5 % by volume. The consistency of the NO_2 content is due to its excessive amount in the reaction mass and a low degree of conversion.

It is necessary to note the difference in the mechanisms of liquid-phase and gas-phase oxidation of CNTs with nitric acid. If in the first case nitrogen oxide (I) is present in the oxidation products only at the initial stage, in the second stage it begins to be produced only in ~2.5 hours after the start of the oxidizing reagent supply in rather small amounts (up to 1.7 % vol.). Moreover, the maximum concentration of N_2O is observed in the oxidation products of the Taunit-M CNTs metal-oxide catalysts that have been refined of impurities, the degree of functionalization of which with oxygen-containing groups was lower than that of the untreated Taunit-M and Taunit-MD CNTs. Proceeding from this, it can be concluded that the catalyst particles, having an accelerating effect on the processes (7), (8), contribute to a decrease in reaction rates (15), (17), (18), (21).

The ratio of the molar proportions of carbon oxides (II) and (IV) in the gaseous products of the interaction of CNTs with nitric acid vapor is in most cases 1: 3. The only exception is the initial period of oxidation of Taunit-M CNT unrefined from catalysts when the reaction products contain more CO.

The data obtained are useful not only for describing the chemistry of the processes that occur. They allow us to estimate molar amounts of gases (per unit mass of CNTs) that require neutralization when this method of oxidizing CNTs in production is realized. Also, the obtained data were used to estimate the total thermal effect and the heating rate of the reaction mass due to it (Table 16). When oxidizing CNTs containing impurities of metal oxide catalysts, the total amount of reaction heat released per unit time is slightly higher than in the oxidation of purified CNTs. This fact is in accordance with the assumption of the catalytic action of inclusions of metal oxides on the process.

Among the processes of gas-phase functionalization, special attention is paid to the production of amidated CNTs by treating the carboxylated nanotubes with gaseous ammonia at elevated temperatures according to scheme:

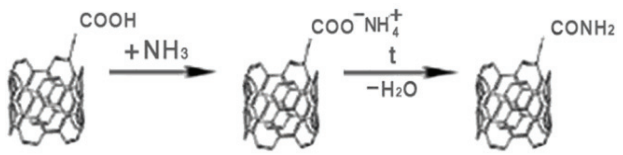

Table 16

The calculated values of the total amount of reaction heat (*qr*) and overheating reagents without taking into account heat losses (*dt*) when oxidizing 1 g of CNTs in concentrated nitric acid vapor at 140 °C

Type of CNT	τ, min	*qr*, J	*dt*, K
Taunit-MD (raw)	90	28.47	5.81
	150	29.57	8.29
	210	26.32	7.40
	270	26.96	7.53
Taunit-M, (raw)	90	15.07	3.01
	150	32.45	9.21
	210	26.37	7.52
	270	24.41	6.98
	360	19.54	4.08
Taunit-M (refined)	150	8.62	3.77
	210	6.45	6.20
	270	6.18	5.97
	360	4.96	3.51

According to the data of XPS-spectroscopy, the carboxylated Taunit-M CNTs, previously treated in ammonia at 250 °C for 10 hours, contained 94.53 at. % of carbon, 4.20 at. % of oxygen, and 1.27 at. % of nitrogen enter. On the unfolded photoelectron spectrum of carbon (Fig. 18*b*), the main peak is identified at 284.4 eV. There is also a peak at 387.9 eV, which confirms the formation of amide groups on the surface of CNTs.

On the photoelectron spectrum of nitrogen (Fig. 18*c*), the most pronounced peak corresponds to a binding energy of about 400 eV, which is typical for atoms in the CONH and NH_2 groups. Some of the nitrogen atoms are quaternary, such as the ones in ammonium salts; they correspond to a peak at 402 eV. Also, the oxidation of N atoms is possible, since the state with a binding energy of about 405 eV O1s oxygen spectra (Fig. 18*d*) is observed broad without an explicit structure. In general, two states with binding energies of 531.5 and 533.3 eV are singled out in them, which correspond to double and single bonds of oxygen atoms with carbon, respectively. The first one corresponds to carbonyl, which is both part of the amide and carboxyl groups, the second one corresponds to the hydroxyl, which can be either an independent surface formation or part of the carboxyl group.

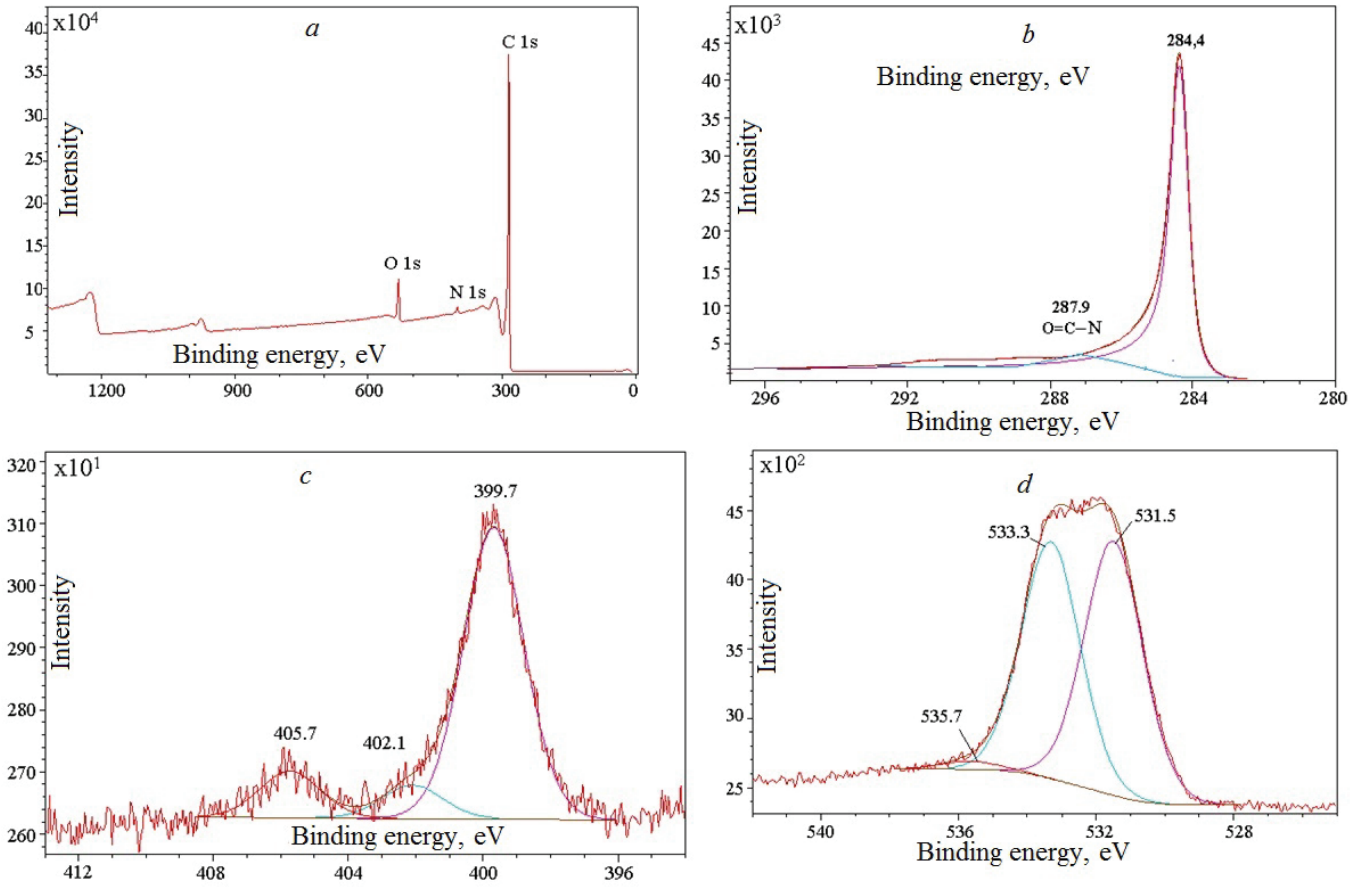

Fig. 18. Panoramic XPS-spectra (*a*) and exploded XRS-spectra for photoelectronic carbon (*b*), nitrogen (*c*) and oxygen (*d*) of Taunit-M after carboxylation and treatment in gaseous ammonia at 250 °C for 10 h

Thus, in the treatment of carboxylated CNTs in ammonia at elevated temperatures, not all COOH groups are converted to amide ones, some of them remain unchanged, some are converted to ammonium groups, some are converted to amide groups. However, 78 % of the nitrogen atoms in the samples, according to the XPS-spectra, are located in the amide groups. Due to this, the action exerted by CNTs treated by this method on polymer matrices differs from the action of the initial and oxidized samples.

Thus, an improvement in a number of physical and mechanical parameters of polymer materials modified with amidated CNTs is shown. In one of the experimental series for the preparation of a composite, a concentrate containing 1.5 % (by weight) of amidated CNTs based on epoxy ED-22 was combined with epoxyaminophenol resin UP-610, followed by curing. The concentration of amidated CNTs in the composite was 0.48 % (by weight). A comparison of the most important characteristics of an unmodified polymer material and a nanocomposite is presented in Table 17.

The introduction of amidated CNTs leads to an increase in viscosity (from 0.4 to 0.58 Pa·s) and a decrease in the gel time (from 34 to 29 min). Also, the composite has a higher (at 16 °C) glass transition temperature, an increase in flexural strength, modulus of elasticity and deflection arrows by 14, 45 and 42 %, respectively. As a rule, when introducing modifying additives into composites, simultaneous growth of mechanical characteristics and glass transition temperature is not possible. However, a result similar to the one obtained has already been observed in the modification of polymer matrices by functionalized CNTs [48–51].

On the basis of amidated CNTs, a polymer structural material (PSM) characterized by increased resistance to impact was also obtained. The analysis of SEM images of the fracture surface of the initial and modified PSM (Fig. 19) shows the change in the adhesion mechanism of destruction along the “matrix-fiber” interface to the cohesive mechanism due to the formation of crosslinks between the functional groups of CNTs and macromolecules of the polymer matrix.

Table 17

Technological, thermal, physical and mechanical properties of the raw polymer material (ED-22 + UP-610) and a composite based on it containing 0.48 % (by weight) of amidated Taunit-M CNTs

Material	Technological properties		Glass transition temperature, °C	Physical and mechanical properties in bending		
	Viscosity at treatment temperature 60 °C, Ps·s	Gel time at 120 °C, min		Ultimate strength, MPa	Modulus of elasticity, MPa	Deflection arrows, mm
Raw polymer	0.40	34	149	140 ± 15.4	2109	6.66
Composite	0.58	29	165	161 ± 11.5	3058	9.51

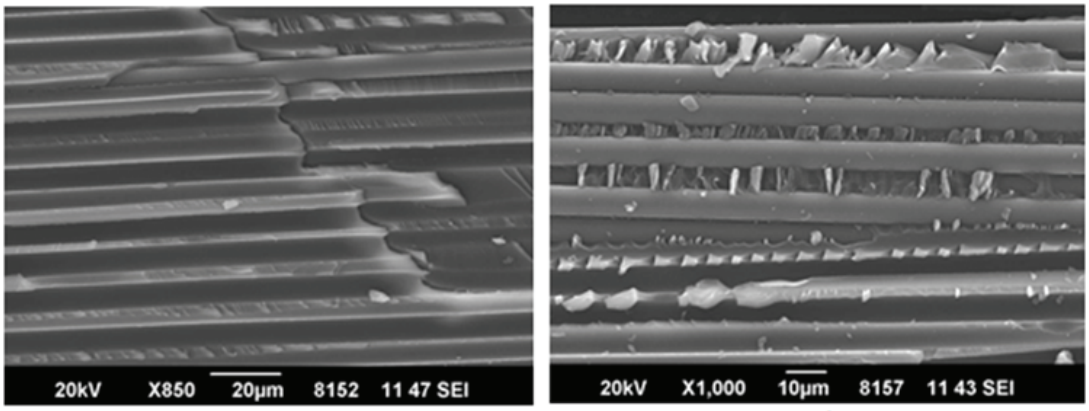

a) *b*)

Fig. 19. The surface of failure as a result of the impact of the initial (*a*) and modified amidated CNT (*b*) of the PSM samples

Thus, the obtained data show a change in the properties of oxidized CNTs after treatment with gaseous ammonia at elevated temperatures and prove the prospects of using this type of functionalized CNTs in the composition of polymer composites.

When designing a device for gas-phase functionalization, it is necessary to ensure the uniformity of the temperature field in the volume of the bulk layer of CNTs. In this case, the non-stationary temperature field of the bulk layer of the processed material is modeled by solving the heat conduction problem for a finite cylinder with a volumetric heat source, which has the following form:

$$\frac{\partial t(x,r,\tau)}{\partial \tau} = a\left(\frac{\partial^2 t(x,r,\tau)}{\partial x^2} + \frac{\partial^2 t(x,r,\tau)}{\partial r^2} + \frac{1}{r}\frac{\partial t(x,r,\tau)}{\partial r}\right) + \frac{q_v}{c\rho}, 0<x<l; \quad 0<r<R; \tag{30}$$

$$t(x,r,0) = f(x,r) - t_{c2}; \tag{31}$$

$$\frac{\partial t(x,0,\tau)}{\partial r} = 0; \tag{32}$$

$$\lambda\frac{\partial t(x,R,\tau)}{\partial r} + \alpha_2\, t(x,R,\tau) = 0; \tag{33}$$

$$\lambda\frac{\partial t(0,r,\tau)}{\partial x} - \alpha_1\left(t(0,r,\tau) - t_{c1} + t_{c2}\right) = 0; \tag{34}$$

$$\lambda\frac{\partial t(l,r,\tau)}{\partial x} + \alpha_3\left(t(l,r,\tau) - t_{c3} + t_{c2}\right) = 0, \tag{35}$$

where $t(x, r, \tau)$ is temperature field of a bounded cylinder as a function of the longitudinal coordinate x, radial coordinate r and time τ; q_v is specific thermal power of a volumetric heat source, J/m^3; λ, c, ρ are thermal conductivity, W/(m·K), heat capacity, J/(kg·K), cylinder material density, kg/m^3, respectively; $f(x, r)$ is initial distribution of temperature; α_1, α_2, α_3 are heat transfer coefficients from the outer surfaces of the cylinder, W/(m^2·K); t_{c1}, t_{c2}, t_{c3} are ambient temperatures from the side of the corresponding surfaces; R, l are radius and height of the cylinder, m, respectively.

The solution of the problem (30)–(35) is used to determine the design and regime parameters of the gas

phase functionalization apparatus, under which the maximum temperature difference over the volume of the bulk CNT layer during the process does not exceed 10 K.

Development of a basic technological procedure for batch production of functionalized forms of carbon nanotubes

The final stage of the work was the development of a chemical-technological scheme for obtaining various forms of functionalized carbon nanotubes based on the regularities of the processes occurring in the work and the results of their mathematical modeling. It seemed expedient to solve this problem using the methodology for designing multi-assortment low-tonnage chemical-technological productions, including those developed at the Tambov State Technical University [52–53].

The final products developed in this procedure (Fig. 20) are prospective for use in various sectors of the art carboxylated CNTs (CCNTs), low functionalized oxidized CNTs (LOCNTs), highly functionalized oxidized CNTs (HOCNTs), amidated CNTs (ACNTs), modified polyaniline CNTs (PANI-CNTs). The possibility of creating a basic procedure is due to the use of similar types of raw materials and general technological methods for its processing; the presence of similar technological stages in the production of different forms of functionalized and modified forms of CNTs, for the implementation of which you can use the same type of equipment.

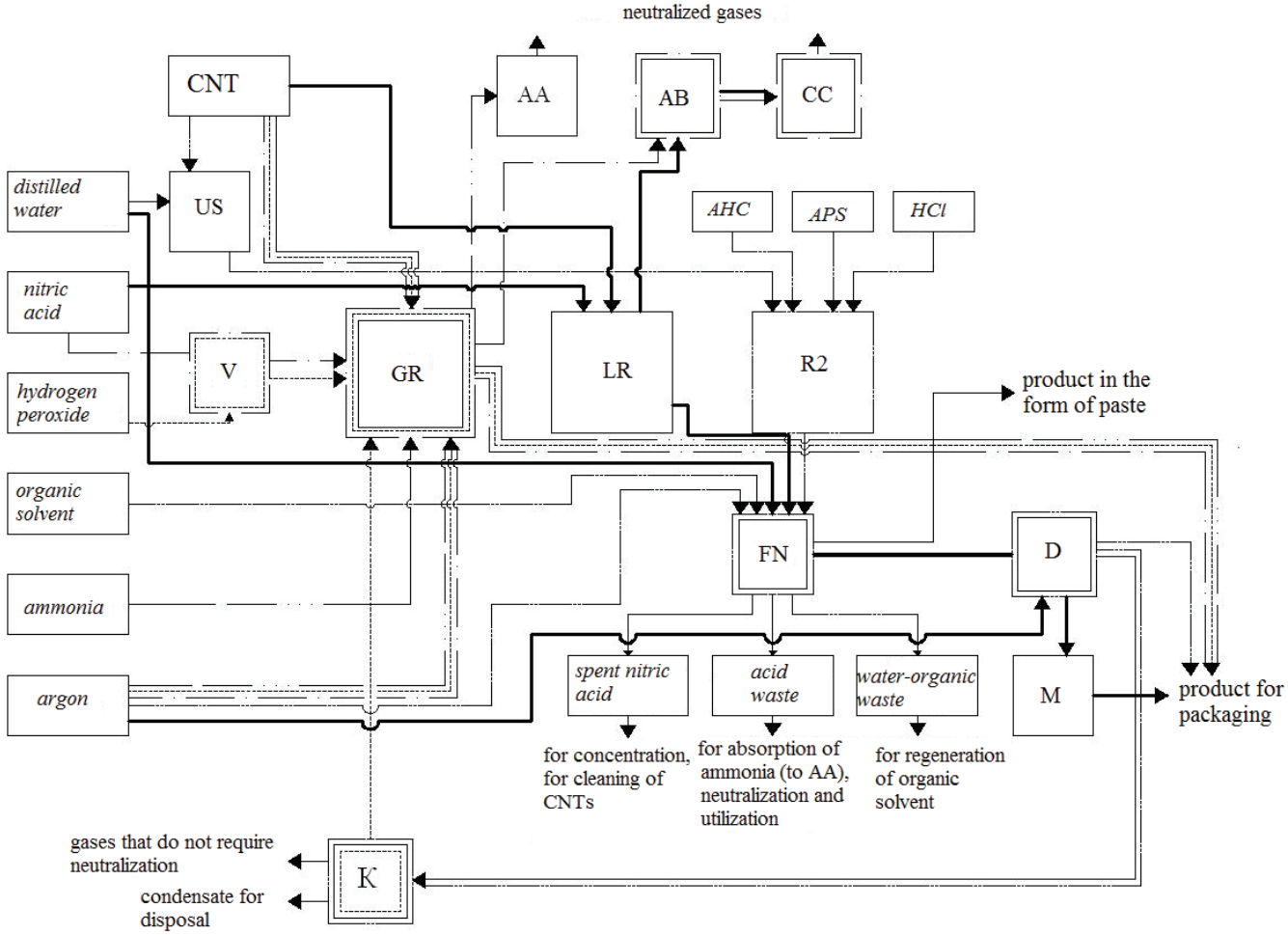

Fig. 20. A sketch of combining the production of various functionalized forms of CNTs in a single technological block diagram.
Types of raw materials and waste are shown in the form of rectangles (abbreviation: *AHC* – aniline hydrochloric acid; *APS* – ammonium persulphate). The most important elements of hardware design are shown in the form of squares (designations: GR – gas phase functionalization apparatus; LR – liquid-phase functionalization apparatus; R2 – oxidative polymerization apparatus; US – ultrasonic unit; AA – ammonia absorber; V – vaporizer; AB – alkaline absorber; CC – catalytic gas cleaning unit; FN – filter neutralizer; D – dryer; M – disintegrator; K – capacitor.
Line designations: ▬ components of the section for preparation of CCNT; ----- – LOCNT; ─ · ─ – HOCNT; – · · · – ACNT; ─-·-─ – PANI-CNT).
The sketch does not show the stages of preliminary preparation of CNT, strengthening of nitric acid and regeneration of organic solvent

For the main reaction equipment of various stages of the basic chemical-process procedure (**CPP**), technological calculations were performed using the developed methods using solutions of equations of mathematical models. The base CPP and the results of technological calculations were transferred as initial data to JSC "ZAVKOM" (Tambov) under contract No. 15051401-NI of May 15, 2014, implemented under the project "Creation of production of polyfunctional carbon nanomaterials and superconcentrates on their basis for use in promising construction polymers and composites of a new generation".

Conclusions

Complex experimental studies of the most important regularities of liquid-phase oxidation processes in various reagent systems have been carried out. The mechanisms of formation of carboxyl groups on the surface of conical and cylindrical CNTs under oxidation by concentrated nitric acid are different. On cylindrical CNTs there is a process consisting of 2 stages of pseudo-first order with different values of effective rate constants. The formation of COOH groups over the entire surface of conical CNTs occurs uniformly and obeys the equations of the formal kinetics of second-order reactions. The calculated values of the effective activation energy indicate a mixed diffusion-kinetic control of the process. Based on the data on the composition of gaseous products of liquid-phase oxidation of CNTs by concentrated nitric acid, a set of chemical reactions is proposed, the presence of which is most likely in this system, and their rates are estimated. The thermal effect of oxidation of CNTs is estimated. A mathematical model of the reactor of liquid-phase oxidative functionalization of CNTs is proposed, which makes it possible to calculate the rational regime and design parameters of equipment for the process.

Gas-phase oxidation in various reagent systems was studied. The advantages of gas-phase processes are shown in a number of cases from the standpoint of saving raw materials and the amount of waste generated. Nanotubes with a minimum content of functional groups and the most qualitative defectiveness indicators were obtained as a result of processing in hydrogen peroxide vapor. Processing in nitric acid vapor and activated ozonization promote deeper oxidation while preserving the morphological features of CNM. The kinetic regularities of CNT oxidation in nitric acid vapor are studied. Differences in the mechanisms of liquid-phase and gas-phase oxidation are shown and the effective values of the rate constant for the formation of carboxyl groups are determined. Effective conditions for the treatment of tubular UMMs in nitric acid vapor have been determined. A mathematical model of the temperature field of a bulk layer of CNTs is proposed for gas-phase processing, calculations using experimental data obtained by kinetic data make it possible to determine the structural and regime parameters of equipment that ensure the necessary qualitative characteristics of functionalized CNTs.

The physicochemical foundations of the processes of functionalization have laid the foundation for a unified scientific approach to the technological realization of the processes of chemical treatment of CNTs in order to obtain products with specified characteristics. The result of application of this approach was a complex technological procedure of batch production of functionalized forms of carbon nanomaterials.

References

1. Zhang B.-T., Zheng X., Li H.-F., Lin J.-M. Application of carbon-based nanomaterials in sample preparation: A review. *Analytica Chimica Acta*, 2013, vol. 784, pp. 1-17.

2. Choudhary N., Hwang S., Choi W. Carbon Nanomaterials: A Review. In: B. Bhushan, D. Luo, S. Schricker, W. Sigmund, S. Zauscher (eds). *Handbook of Nanomaterials Properties*. Springer, Berlin, Heidelberg, 2014, pp. 709-769. https://doi.org/10.1007/978-3-642-31107-9_37.

3. Xu J., Cao Z., Zhang Y., Yuan Z. et al. A review of functionalized carbon nanotubes and grapheme for heavy metals adsorption from water: Preparation, application and mechanism. *Chemosphere*, 2018, vol. 195, pp. 351-364.

4. Thines R.K., Mubarak N.M., Nizamuddin S., Sahu J.N. et al. Application potential of carbon nanomaterials in water and wastewater treatment: A review. *Journal of the Taiwan Institute of Chemical Engineering*, 2017, vol. 72, pp. 116-133.

5. Apul O.G., Karanfil T. Adsorption of synthetic organic contaminants by carbon nanotubes: A critical review. *Water Research*, 2015, vol. 68, pp. 34-55.

6. Chesnokov V.V., Podyacheva O.Yu., Richards R.M. Influence of carbon nanomaterials on properties of Pd/C catalysts in selective hydrogenation of acetylene. *Materials Research Bulletin*, 2017, vol. 88, pp. 78-84.

7. Gao M., Jiang N., Zhao Y., Xu C. et al. Copper-cerium oxides supported on carbon nanomaterial for preferential oxidation of carbon monooxide. *Journal of Rare Earth*, 2016, vol. 34, pp. 55-60.

8. Xu Z.-L., Kim J.-K., Kang K. Carbon nanomaterials for advanced lithium sulfur batteries. *Nanotoday*, 2018, vol. 19, pp. 84-107.

9. Zhang Y., Jiao Y., Liao M., Wang B. et al. Carbon nanomaterials for flexible lithium ion batteries. *Carbon*, 2017, vol. 124, pp. 79-88.

10. Liu L., Niu Z., Chen J. Flexible supercapacitops based on carbon nanotubes. *Chinese Chemical Letters*, 2018, vol. 29, pp. 571-581.

11. He S., Hu Y., Wan J., Gao Q. et al. Biocompatible carbon nanotube fibers for implantable supercapacitors. *Carbon*, 2017, vol. 122, pp. 162-167.

12. Yoo Y.-E., Park J., Kim W. Understanding and controlling the rest potential of carbon nanotube based supercapacitors for energy density enhancement. *Applied Surface Science*, 2018, vol. 433, pp. 765-771.

13. Zhai W., Srikanth N., Kong L.B., Zhou K. Carbon nanomaterials in tribology. *Carbon*, 2017, vol. 119, pp. 150-171.

14. Tarfaoui M., Lafdi K., El Moumen A. Mechanical properties of carbon nanotubes based polymer composites. Composites Part B: Engineering, 2016, vol. 103, pp. 113-121.

15. Yamamoto T., Kawaguchi K. Synthesis of composite polymer particles with carbon nanotubes and evaluation of their mechanical properties. *Colloids and Surfaces A: Physicochemical and Engineering Aspects*, 2017, vol. 529, pp. 765-770.

16. Patil A., Patel A., Sharma P.K. Effect of carbon Nanotube on Mechanical properties of Hybrid Polymer Matrix nanocomposites at Different Weight Percentages. *Materials Today Proceedings*, 2018, vol. 5, issue 2(1), pp. 6401-6405.

17. Song H., Qiu Y., Wang Y., Cai K. et al. Polymer/carbon nanotube composite materials for flexible thermoelectric power generator. *Composite Science and Technology*, 2017, vol. 153, pp. 71-83.

18. Ji T., Feng Y., Qin M., Feng W. Thermal conducting properties of aligned carbon nanotubes and their polymer composites. *Composites Part A: Applied Science and Manufacturing*, 2016, vol. 91, pp. 351-369.

19. Cen-Puc M., Oliva-Alives A. I., Alives F. Thermoresistive mechanisms of carbon nanotube / polymer composites. *Physica E: Low-dimensional Systems and Nanostructures*, 2018, vol. 96, pp. 41-50.

20. Ia Z., Ma H.-I., Cheng L.-K., Lau K.-T. et al. Stress transfer properties of carbon nanotube reinforced polymer composites at low temperature environments. *Composites Part B: Engineering*, 2016, vol. 106, pp. 356-365.

21. Jackson E.M., Laibinis P.E., Collins W.E., Ueda A. et al. Development and thermal properties of carbon nanotube – polymer composites. *Composites Part B: Engineering*, 2016, vol. 89, pp. 362-373.

22. Fontananova E., Grosso V., Aljlil S.A., Bahattab M.A. et al. Effect of functional groups on the properties of multiwalled carbon nanotubes/polyvinilidenfluoride composite membranes. *Journal of Membrane Science*, 2017, vol. 541, pp. 198-204.

23. Ferreira F.V., Franceschi W., Menezes B.R.C., Brito F.S. et al. Dodecylamine functionalization of carbon nanotubes to improve dispersion, thermal and mechanical properties of polyethylene based nanocomposites. *Applied Surface Science*, 2017, vol. 410, pp. 267-277.

24. Kuang Y., Huang B. Effects of covalent functionalization on the thermal transport in carbon nanotube/polymer composites: A multiscale investigaation. *Polymer*, 2015, vol. 56, pp. 563-571.

25. Xiao T., Liu J., Xiong H. Effects of different functionalization schemes on the interfacial strength of carbon nanotube polyethilene composite. *Acta mechanica Solida Sinica*, 2015, vol. 28, pp. 277-284.

26. Alam A., Zhang Y., Kuan H.-C., Lee S.-H. et al. Polymer composite hydrogels containing carbon nanomaterials – morphology and mechanical and functional performance. *Progress in Polymer Science*, 2018, vol. 77, pp. 1-18.

27. Liu X., Xu F., Zhang K., Wei B. et al. Characterization of enhanced interfacial bonding between epoxy and plasma functionalized carbon nanotube films. *Composites Science and Technology*, 2017, vol. 145, pp. 114-212.

28. Punetha V.D., Rana S., Yoo H.J., Haurasia A. et al. Functionalization of carbon nanomaterials for advanced polymer nanocomposites. A comparison study between CNT and grapheme. *Progress in Polymer Science*, 2017, vol. 67, pp. 1-47.

29. Rukhov A.V., Bakunin E.S., Burakova E.A., Besperstova G.S. et. al. Features of technology of preparation of catalytic systems by thermal decomposition for synthesis of carbon nanotubes. *Inorganic Materials: Applied Research*, 2017, vol. 8, pp. 802-807.

30. Chen J., Chen Q., Ma Q., Li Y. et al. Chemical treatment of CNTs in acidic $KMnO_4$ solution and promoting effects on the corresponding Pd-Pt/CNTs catalyst. *Journal of Molecular Catalysis A: Chemical*, 2012, vol. 356, pp. 114-120.

31. Boehm H.P. Chemical identification of surface groups. *Advances in catalysis and related subjects*, 1996, vol. 16, pp. 179-274.

32. Patent 2528985 RF, V82V3/00 C01V31/02 Sposob modificirovaniya uglerodnyh nanotrubok [Method for modifying carbon nanotubes] Tkachev A.G., Melezhik A.V., Dyachkova T.P., Aladinskij A.A.; Appl. 03.07.2012; publ. 20.09.2014. (Rus)

33. Yu H., Jin Y., Peng F. et al. Kinetically Controlled Side-Wall Functionalization of Carbon Nanotubes by Nitric Acid Oxidation. *Journal of Physical Chemistry C*, 2008, vol. 112, pp.6758-6763.

34. Savilov S.V., Ivanov A.S., Chernyak S.A. et al. Features of the oxidation of multiwalled carbon nanotubes. Russian Journal of Physical Chemistry A, 2015, vol. 89, pp. 1989-1996.

35. Da Silva A.M., Dos Santos H.F., Giannozzi P. Carbonyl group generation on single-wall carbon nanotubes with nitric acid: A theoretical description. *Chemical Physics Letters*, 2013, vol. 582, pp. 123-128.

36. Gerber I., Oubenali M., Bacsa R., Durand J. et al. Theoretical and Experimental Studies on the Carbon-Nanotube Surface Oxidation by Nitric Acid: Interplay

between Functionalization and Vacancy Enlargement. Chemical European Journal, 2011, vol. 17, pp. 11467-11477.

37. Kirchner U., Scheer V., Vogt R. FTIR Spectroscopic Investigation of the Mechanism and Kinetics of the Heterogeneous Reactions of NO_2 and HNO_3 with Soot. *Journal of Physical Chemistry A*, 2000, vol. 104, pp. 8908-8915.

38. Stanmore B.R., Tschamber V., Brilhac J.-F. Oxidation of carbon by NOx, with particular reference to NO_2 and N_2O. Fuel, 2008, vol. 87, pp. 131-146.

39. Forsman W.C., Vogel F.L., Carl D.E., Hoffman J.Chemistry of graphite intercalation by nitric acid. Carbon, 1978, vol. 16, pp. 269-271.

40. Dyachkova T.P., Han Yu. A., Orlova N.V., Kondrashov S.V. Okislenie mnogoslojnyh uglerodnyh nanotrubok v parah perekisi vodoroda: zakonomernosti i ehffekty. *Vestnik Tambovskogo gosudarstvennogo tekhnicheskogo universiteta* [Transactions of TSTU], 2016, vol. 22, issue 2, pp. 323 – 333.

41. Zhang Z., Atkinson J.D., Jiang B. et al. Nitric oxide oxidation catalyzed by microporous activated carbon fiber cloth: An updated reaction mechanism. Applied Catalysis B: Environmental, 2014, vol. 148-149, pp. 573-581.

42. Setiabudi A., Makkee M., Moulijn J.A. The role of NO_2 and O_2 in the accelerated combustion of soot in diesel exhaust gases. *Applied Catalysis B: Environmental*, 2004, vol. 50, pp. 185-194.

43. Kalberer M., Talbor K., Ammann M.et al. Heterogeneous Chemical Processing of $^{13}NO_2$ by Monodisperse Carbon Aerosols at Very Low Concentrations. *Journal of Physical Chemistry*, 1996, vol. 100, pp. 15487-15493.

45. Yagud B.Y., Amirova S.A., Kefer R.G. et al. The reaction of nitrogen dioxide and nitrosyl chloride with activated charcoal. *Russian Journal of Inorganical Chemistry*, 1971, vol. 16, pp. 792-794.

46. Chugtai A.R., Atteya M.M., Kim J. et al. Adsorption and adsorbate interaction at soot particle surfaces. *Carbon*, 1998, vol. 36, pp. 1573-1589.

47. Hou P., Liu C., Tong Y. et al. Purification of single-walled carbon nanotubes synthesized by the hydrogen arc-discharge method. *Journal of Materials Research*, 2001, vol. 16, pp. 2526-2529.

48. Jeguirim M., Tschamber V., Brilhac J.F., Ehrburger P. Oxidation mechanism of carbon black by NO_2: Effect of water vapour. *Fuel*, 2005, issue 14-15, pp. 1949-1956.

49. Sui G., Zhona W.H., Liu M.C., Wu P.H. Enhancing mechanical properties of an epoxy resin using "liquid nano-reinforcements". *Materials Science and Engineering* A, 2009, vol. 512, pp. 139-142.

50. Kim J.T., Kim H.-C., Kim S.-K., Kathi J. 3-aminopropyltriethoxysilane effect on thermal and mechanical properties of multi-walled carbon nanotubes reinforced epoxy composites. *Journal of composite materials*, 2009, vol.43, pp. 2533-2541.

51. Wang S., Liang R., Liu T., Wang B., Zhang C. Covalent addition of diethyltoluenediamines onto carbon nanotubes for composite application. *Polymer composites*, 2009, vol. 30, pp.1050-1057.

52. Malygin E.N., Karpushkin S.V., Krasnyan-skiy M.N., Ostroukh A.V. Technical equipment configuration and functioning mode optimizing for chemical-engineering systems of multi-product plants. *American Eurasian Journal of Agricultural and Environmental Sciences*, 2015, vol. 15, pp. 447.

53. Malygin E.N., Karpushkin S.V., Borisenko A.B. A mathematical model of the functioning of multiproduct chemical engineering systems. *Theoretical Foundations of Chemical Engineering*, 2005, vol. 39, pp. 429-439.